1-1-2010

The lisa gravitational wave foreground: A study of double white dwarfs

Ashley J. Ruiter

Krzysztof Belczynski

Matthew Benacquista

Shane L. Larson

Gabriel Williams

Recommended Citation

THE *LISA* GRAVITATIONAL WAVE FOREGROUND: A STUDY OF DOUBLE WHITE DWARFS

Ashley J. Ruiter[1,2,3], Krzysztof Belczynski[4,5,9], Matthew Benacquista[6], Shane L. Larson[7], and Gabriel Williams[6,8]

[1] Max-Planck-Institut für Astrophysik, Karl-Schwarzschild-Str. 1, 85741 Garching, Germany; ajr@mpa-garching.mpg.de
[2] Harvard-Smithsonian Center for Astrophysics, 60 Garden St., Cambridge, MA 02138, USA
[3] New Mexico State University, Department of Astronomy, 1320 Frenger Mall, Las Cruces, NM 88003, USA
[4] Los Alamos National Laboratory, CCS-2/ISR-1 Group, P.O. Box 1663, Los Alamos, NM 87545, USA; kbelczyn@nmsu.edu
[5] Astronomical Observatory, University of Warsaw, Al. Ujazdowskie 4, 00-478 Warsaw, Poland
[6] Center for Gravitational Wave Astronomy, The University of Texas at Brownsville, 80 Fort Brown, Brownsville, TX 78520, USA; benacquista@phys.utb.edu,
gabriel.j.williams@gmail.com
[7] Department of Physics, Utah State University, 4415 Old Main Hill, Logan, UT 84322, USA; s.larson@usu.edu
[8] Department of Atmospheric Science, Colorado State University, 200 West Lake Street, Fort Collins, CO 80523

ABSTRACT

Double white dwarfs (WDs) are expected to be a source of confusion-limited noise for the future gravitational wave observatory *LISA*. In a specific frequency range, this "foreground noise" is predicted to rise above the instrumental noise and hinder the detection of other types of signals, e.g., gravitational waves arising from stellar-mass objects inspiraling into massive black holes. In many previous studies, only detached populations of compact object binaries have been considered in estimating the *LISA* gravitational wave foreground signal. Here, we investigate the influence of compact object detached and Roche-Lobe overflow (RLOF) Galactic binaries on the shape and strength of the *LISA* signal. Since >99% of remnant binaries that have orbital periods within the *LISA* sensitivity range are WD binaries, we consider only these binaries when calculating the *LISA* signal. We find that the contribution of RLOF binaries to the foreground noise is negligible at low frequencies, but becomes significant at higher frequencies, pushing the frequency at which the foreground noise drops below the instrumental noise to >6 mHz. We find that it is important to consider the population of mass-transferring binaries in order to obtain an accurate assessment of the foreground noise on the *LISA* data stream. However, we estimate that there still exists a sizeable number (∼11,300) of Galactic double WD binaries that will have a signal-to-noise ratio >5, and thus will be potentially resolvable with *LISA*. We present the *LISA* gravitational wave signal from the Galactic population of WD binaries, show the most important formation channels contributing to the *LISA* disk and bulge populations, and discuss the implications of these new findings.

Key words: binaries: close – gravitation – gravitational waves – stars: evolution – white dwarfs

Online-only material: color figure

1. INTRODUCTION

To obtain important information about a variety of astrophysical sources, astrophysics must move toward observations beyond the electromagnetic spectrum. Several ground-based gravitational radiation (GR) observatories are already working at full efficiency and collecting data (e.g., The LIGO Scientific Collaboration (LIGO); Abbott 2007). These detectors are sensitive in a high GR frequency regime (above a few tens of Hertz), where signals are expected to come from mergers of compact stellar-mass objects like neutron stars (NSs) and black holes (BHs). However, these types of events are infrequent, their rate estimates are burdened with heavy uncertainties (e.g., Belczynski et al. 2002; Kalogera et al. 2004; O'Shaughnessy et al. 2008), and it is not clear whether any merger detections are likely given the current level of instrument sensitivity (Abbot et al. 2009). The future generation of GR detectors includes *LISA*, the Laser Interferometer Space Antenna (Danzmann 1996; Hughes 2006, and references therein), a joint ESA and NASA mission. It is a space-based all-sky interferometer which will be more sensitive to lower frequencies[10] (∼10^{-4}–0.1 Hz) than ground-based GR detectors are. The different frequency regimes will allow for the observations of sources of a different nature. The most promising sources for *LISA* are mergers of supermassive and/or intermediate-mass BHs (i.e., Sesana et al. 2005), extreme mass ratio inspirals (EMRIs; e.g., Gair 2009) of stellar-mass objects into supermassive BHs, and stellar-mass compact remnant binaries (see, e.g., Hils et al. 1990; Benacquista et al. 2007).

At first, it was believed that contact W UMa systems (Mironovskii 1965) would dominate the GR signal in the low-frequency range, but later works (e.g., Evans et al. 1987; Lipunov et al. 1987; Hils et al. 1990) have shown that close double white dwarf (WD) binaries are more important at low frequencies, and are a guaranteed source of gravitational waves for *LISA*. The gravitational wave signal arising from double WDs in the Galaxy will put constraints on the star formation history of the Milky Way (MW), as well as the scale height and shape of the thick disk and Galactic bulge (Benacquista & Holley-Bockelmann 2006).

The Galactic double WDs will contribute to the *LISA* signal as both unresolved and resolved sources. At low frequencies (≲3 mHz; pertaining to binaries with orbital periods larger than 11 minutes), predicted binary numbers are so high that most of the GR signals from individual systems will be unresolved, and they will form a confusion-limited "foreground" noise. Within that frequency range, only GR sources that are relatively close to the detector or are strong GR emitters will stand out above the foreground noise. At higher frequencies (≳3 mHz; orbital

---

[9] Oppenheimer Fellow.
[10] For a circular binary, f_{gr} (Hz) = 2/(orbital period) (s).

periods <11 minutes), the numbers of double WDs are relatively small and thus they are expected to be resolved, offering an opportunity to study uncertain parameters associated with binary evolution and WD physics (e.g., possible progenitors of SNe Ia and R CrB stars). *LISA* will be mostly sensitive to Galactic stellar-mass binaries; however, a small contribution from extragalactic systems is also predicted (Hils et al. 1990; Kosenko & Postnov 1998; Farmer & Phinney 2003). The gravitational wave radiation from coalescing double WDs was investigated using smoothed particle hydrodynamics by Lorén-Aguilar et al. (2005). It is expected that the signal arising from merging double WDs would be detectable prior to the coalescence, though would not contribute significantly to the *LISA* gravitational wave signal overall, as the Galactic double WD merger event rate is predicted to be as low as ∼1 per century (Nelemans et al. 2001b).

Among the objects that are expected to be important verification sources for *LISA* are the compact AM Canum Venaticorum (AM CVn) binaries (see Roelofs et al. 2007a for gravitational wave strain amplitude estimates of five known AM CVn binaries). AM CVn systems are a sub-class of cataclysmic variables with $\lesssim$1 hr orbits in which a WD accretes matter via Roche-Lobe overflow (RLOF) from what is believed to be a helium-rich WD or a (semi-degenerate) helium star (Smak 1967; Warner 1995a; Nelemans et al. 2001a). These close binaries are faint and thus not readily detected electromagnetically, but are expected to be observable in gravitational waves (25 AM CVn systems have been confirmed to date).[11]

Besides double WD binaries, other close compact binaries including NSs and BHs have been studied by other groups (e.g., Nelemans et al. 2001b; Cooray 2004). Some few tens of these systems with orbital periods within the *LISA* sensitivity range are known in the Galaxy. There are also $\gtrsim$8 ultracompact X-ray binaries, which consist of a WD transferring matter through RLOF to an NS on ∼40 minute orbits (Wang & Chakrabarty 2004). Double NSs are also known, however, only one such system is observed with a period (of 2.4 hr) within the *LISA* sensitivity range (Burgay et al. 2003). Close binaries with BHs (like BH–BH, BH–NS, and BH–WD) have yet to be observed, but they are predicted to populate the Galaxy in smaller numbers than systems with NSs and/or WDs.

Previous work on Galactic compact binary populations in the context of *LISA* has been done with the exclusion of RLOF systems (Hils et al. 1990; Postnov & Prokhorov 1998; Benacquista et al. 2004; Timpano et al. 2006) or with the entire RLOF + detached populations combined (Nelemans et al. 2001b; Edlund et al. 2005). In addition, Hils & Bender (2000) studied AM CVn systems separately using an analytical approach, finding no significant increase in the confusion-limited noise for space-based GR detectors with the addition of RLOF binaries, while Nelemans et al. (2004) calculated the GR amplitude of resolved WD binaries using population synthesis methods (both detached and AM CVn systems), finding that *LISA* would resolve a total of 22,000 Galactic double WDs (∼11,000 detached and 11,000 AM CVn). However, a more recent study that takes into account the local space density of AM CVn stars predicts that only ∼10^3 AM CVn binaries will be resolved with *LISA* (Roelofs et al. 2007b). This estimate is still ∼2 orders of magnitude above the current number of AM CVn systems that have so far been detected.

In modeling our stellar population, we use an updated population synthesis method with recent results on mass transfer/accretion in compact object binaries, and which is significantly different and more complex than the methods used in previous calculations. In this study, we assess the importance of detached and RLOF compact binary populations in the Galactic disk and bulge on the overall *LISA* sensitivity. In Section 2, we describe our binary modeling techniques and signal calculations; in Section 3 we show the physical properties (masses and orbital periods) of our double WD population, and show the most important evolutionary channels that contribute to the overall *LISA* signal arising from the four Galactic sub-populations (detached disk, RLOF disk, detached bulge, and RLOF bulge). In Section 4, we show the *LISA* GR signals, estimate the likelihood of source resolvability, and comment on the detectability and selection effects of the potentially resolvable systems within our Galaxy. In Section 5, we compare our results with those of previous studies, and in Section 6 we give a summary of our findings.

2. MODEL DESCRIPTION

2.1. Population Synthesis Model

In this study, the combined Galactic population of RLOF and detached compact remnant binaries with orbital periods spanning the *LISA* band is considered. We use the StarTrack population synthesis code described in detail in Belczynski et al. (2008b) to evolve primordial binaries within the Galaxy from the zero-age main sequence (ZAMS) and calculate their properties. The code has undergone a number of important updates since Belczynski et al. (2002), including detailed mass-transfer calculations. Recent results on mass accumulation in the context of ultracompact X-ray binary formation are given in Belczynski & Taam (2004), while those for double WD binaries are given in Belczynski et al. (2005).

We evolve the field population of single and binary stars (50% binarity) with solar-like metallicity ($Z = 0.02$). Single star evolution is followed from the ZAMS employing modified analytic formulae and evolutionary tracks from Hurley et al. (2000). For the evolution of binary stars, the calculations also include full orbital evolution with tidal interactions, magnetic braking, supernova natal kicks, and GR emission (see Belczynski et al. 2008b, for formulae). ZAMS masses ($M_{\rm ZAMS}$) span the mass range 0.08–100 $M_\odot$. Single stars and binary primaries ($M_{\rm a}$) are drawn from a three-component broken power law initial mass function (Kroupa et al. 1993), and secondary masses ($M_{\rm b}$) are obtained from a flat mass ratio distribution q = secondary/primary (e.g., Mazeh et al. 1992). We note as well that binary interactions leading to mass-transfer events may alter the course of evolution for stars of a given initial mass. Initial orbital separations span a wide range up to 10^5 $R_\odot$ and are drawn from a distribution that is flat in the logarithm, while initial eccentricities are taken from a thermal-equilibrium eccentricity distribution (see Abt 1983; Duquennoy & Mayor 1991). Progenitors of all binaries are initially formed on eccentric orbits. Tidal interactions between binary components circularize orbits before the first RLOF in a given progenitor system occurs. However, for a small fraction (10%) of double WD progenitors that are initially found on very eccentric orbits, the first RLOF is encountered when the orbit is still eccentric. In such a case, we assume an instant circularization at periastron ($a_{\rm new} = a_{\rm old} (1 − e_{\rm old})$ and $e_{\rm new} = 0$), and follow with the RLOF calculation. At the time of double WD formation, all of the orbits are circular. Eccentric WD binaries are expected to arise from dynamical interactions

---

[11] http://www.astro.ru.nl/∼nelemans/dokuwiki/doku.php?id=verification_binaries:am_cvn_stars

in globular clusters (Benacquista 2001), and though we do not consider them here, could provide a unique opportunity for learning about WD structure with *LISA* (Willems et al. 2008).

For the population of Galactic disk binaries, we use a continuous star formation rate for 10 Gyr, while for the bulge population we use a constant star formation rate for the first Gyr, and no star formation thereafter (entire MW age is 10 Gyr). This translates to a present Galactic star formation rate of 4 $M_\odot$ yr^{-1} (disk mass = $4 \times 10^{10}\,M_\odot$ with a constant star formation rate for 10 Gyr = 4 $M_\odot$ yr^{-1}; see Section 2.2), which is within reasonable agreement with the current Galactic star formation rate estimate of 3.6 $M_\odot$ yr^{-1} (Cox 2000). We note however that it has been suggested that the star formation rate of the MW has been (mostly) decreasing exponentially with time, only reaching $\sim 3.6\,M_\odot$ yr^{-1} at the current epoch (Nelemans et al. 2001b, 2004, see Section 2.2), with the integrated mass in formed stars being closer to $8 \times 10^{10}\,M_\odot$. Since the star formation history of the MW disk and bulge is not precisely known, we choose to model the Galaxy with simple star formation histories (1 Gyr-long "continuous burst" (bulge), and constant for 10 Gyr (disk)), which to first order is a reasonable representation of the global star formation history of the Galaxy.

The most uncertain phase in close binary evolution affecting the orbital separation for low- and intermediate-mass stars is the common envelope (CE) phase (Postnov & Yungelson 2006). Close binaries are expected to go through at least one CE event, and there are currently a few prescriptions of CE evolution in the literature (Webbink 1984; Nelemans & Tout 2005; van der Sluys et al. 2006; Beer et al. 2007). In our simulations, the CE phase is treated using energy balance as discussed in Webbink (1984), in which the orbital energy of the binary is diminished at the expense of the unbinding of the donor envelope. The post-CE separation is governed by the parameters λ (de Kool 1990), a function of the donor's structure, and the highly uncertain α, the efficiency with which the binary orbital energy is used to unbind the envelope. We have chosen to use $\alpha \times \lambda = 1$. The effects of using other CE efficiencies have not been fully explored here, though lower CE efficiencies result in closer post-CE binaries, and a higher number of stellar mergers.

At the current age of the Galaxy (10 Gyr), we extract all binaries containing two compact remnants: WDs, NSs, and BHs in the gravitational frequency range: 0.0001–1 Hz, which encompasses the *LISA* sensitivity range (orbital periods of 5.6 hr–2 s). Henceforth when we refer to "*LISA* binaries," we are referring to binary systems in our study within this GR frequency band. As previously stated, we consider only WD binaries when calculating the *LISA* signal. There are five types of WDs considered in the evolution: helium (He WD), formed by stripping the envelope off a Hertzsprung gap or red giant low-mass star; carbon–oxygen (CO WD), formed from progenitors with masses ~ 0.8–6.3 $M_\odot$; oxygen–neon (ONe WD), formed from progenitors with masses ~ 6.3–8.0 $M_\odot$; hybrid (Hyb WD), having a CO-core and an He-envelope, formed via the stripping of the envelope from a helium burning star, and hydrogen (H WD), formed by stripping the envelope from a very low mass ($\lesssim 0.8\,M_\odot$) main sequence (MS) star. In our *LISA* GR calculations, we only consider the first four types of WDs, as hydrogen WDs are more representative of brown dwarf (BD) like objects and thus we will from now on refer to them as BDs. For the current study, the BDs (formed through binary evolution) do not play a large role in contributing to the *LISA* GR signal due to their low mass (see Section 5). We note, however, that in older stellar populations, the fraction of binaries that contain

H WDs becomes more significant (see Ruiter et al. 2009 for the calculation of the *LISA* signal from MW halo double WDs, which includes "hydrogen WDs").

In compact binaries, gravitational wave emission is a strong source of angular momentum loss. The average rate of orbital angular momentum loss due to GR for $e = 0$ binaries is calculated from Peters (1964):

$$\frac{dJ_{\rm gr}}{dt} = \frac{-32}{5} \frac{G^{7/2}\,M_{\rm p}^2\,M_{\rm s}^2\,\sqrt{M_{\rm p} + M_{\rm s}}}{c^5\,a^{7/2}}, \qquad (1)$$

where G is the gravitational constant and c is the speed of light. At every time step in our calculations, the evolving system is checked for RLOF. Upon reaching contact (RLOF), we assume that mass-transfer is GR-driven and the donor ($M_{\rm don}$) mass-transfer rate is calculated via

$$\dot{M}_{\rm don} = M_{\rm don} D^{-1} \frac{dJ_{\rm gr}/dt}{J_{\rm orb}}, \qquad (2)$$

where RLOF stability is determined by the parameter D (see, e.g., King & Kolb 1995)

$$D = \frac{5}{6} + \frac{1}{2}\zeta_{\rm don} - \frac{1 - f_{\rm a}}{3(1 + q)} - \frac{(1 - f_{\rm a})(1 + q)\beta_{\rm mt} + f_{\rm a}}{q}. \qquad (3)$$

$J_{\rm orb}$ is the orbital angular momentum of the binary, $f_{\rm a}$ is the fraction of transferred mass accreted by the WD of mass $M_{\rm acc}$ ($f_{\rm a} = 1$ for stable RLOF), $q \equiv (M_{\rm acc}/M_{\rm don})$, and $\beta_{\rm mt} = M_{\rm don}^2/(M_{\rm don} + M_{\rm acc})^2$. The radius mass exponent for the donor $\zeta_{\rm don}$ is obtained from stellar models in each time step (see Belczynski et al. 2008b) and is ~ -0.35 for WD donors in a phase of stable mass transfer. Stable RLOF between two WDs leads to an increase in orbital period where dynamically unstable RLOF leads to a merger. See Belczynski et al. (2008b) for a more detailed description of treatment of mass transfer/ accretion phases in StarTrack.

2.2. Calibration and Spatial Distribution of Sources

In our simulations, both the detached and RLOF systems have been distributed between the disk and bulge separately, assuming no correlation between the position and age of the system. For the current study, we have neglected the halo population of double WDs, but these systems have been investigated in another work (Ruiter et al. 2009). The density distribution of the Galactic disk is taken to have the following form

$$\rho(\mathbf{R}, \mathbf{z}) = \frac{N_d}{4\pi R_0^2 z_0} e^{-R/R_0} e^{|-z|/z_0} \qquad (4)$$

in cylindrical coordinates, and the density distribution of the bulge has the form

$$\rho(\mathbf{r}) = \frac{N_b}{4\pi r_0^3} e^{-(r/r_0)^2} \qquad (5)$$

in spherical coordinates (bulge scale length $r_0 = \sqrt{x^2 + y^2 + z^2}$).

N_d and N_b represent the total number of simulated double WDs in the disk and bulge, respectively. We have calibrated our results using stellar Galactic disk and bulge masses from Klypin et al. (2002), with masses of $4 \times 10^{10}\,M_\odot$ and $2 \times 10^{10}\,M_\odot$, respectively. We have chosen $R_0 = 2500$ pc and $z_0 = 200$ pc for the disk scale length and scale height, while $r_0 = 500$ pc with a radial cutoff of 3500 pc for the bulge (Nelemans 2003a).

While we note that even a scale height of 500 pc would be a reasonable choice for disk WDs (Majewski & Siegel 2002), we have chosen to use 200 pc so that our results are more readily comparable to those of previous studies (Nelemans et al. 2001b; Benacquista & Holley-Bockelmann 2006).

Our original *LISA* double WD binaries, which were born directly from `StarTrack` (8.4×10^4), were the result of the evolution of 20×10^6 ZAMS binaries. Since evolving the whole Galactic population of *LISA* binaries is time intensive, an interpolation scheme was developed in order to scale our number of `StarTrack` binaries to match those of the MW bulge and disk by stellar mass. Probability distribution functions (PDFs) were constructed for different evolutionary channels as a function of the primary and secondary masses and GR frequency. For RLOF binaries, it was only necessary to construct PDFs as a function of the masses since the orbital period, and hence GR frequency, was then uniquely determined by the masses. We chose to construct PDFs (instead of simply scaling the original binaries by a factor of $\gtrsim 300$) so that our systems would span a range of frequencies and masses pertinent to said formation channel. The PDFs were constructed using a kernel density estimator that best replicated the characteristics of the population (Williams 2008). The KDE package for Matlab was used to generate the specific PDFs. This technique was particularly successful for well-populated evolutionary channels, where we could be sure that the range of masses and frequencies was well covered. For some of the least-populated channels, the full range of binary masses and frequencies was not covered sufficiently to yield a smooth extrapolation of the data. Thus, apparent clumps of binaries that are comparable in number to our scaling factors are attributable to an undersampling of the frequency and mass range for these rare evolutionary channels.

2.3. LISA Signal Calculations

The gravitational wave signal from the *LISA* data stream will be a time delay interferometry (TDI) variable in which the phases of the laser signals at each vertex of *LISA* are combined with the phases of other signals at delayed times in order to reduce the laser phase noise and accommodate the varying armlengths of the constellation of the spacecraft (Rubbo et al. 2004). At low frequencies, the signal at any given vertex can be very well approximated by the Michelson signal:

$$h(t) = \frac{1}{2} h_{ab} \left(\ell_1^a \ell_1^b - \ell_2^a \ell_2^b \right), \tag{6}$$

where h_{ab} is the wave metric and ℓ_1 and ℓ_2 are the unit vectors pointing along the two arms that join at the vertex. The transfer frequency is the frequency at which point the GR wavelength becomes comparable to the armlength of *LISA*. For high (e.g., above the transfer frequency) GR frequencies, the period of the gravitational wave is then less than the time it takes for light to propagate between the *LISA* spacecraft detectors, and the low-frequency approximation breaks down. The transfer frequency is given by $f_* = c/(2\pi L) \approx 0.01$ Hz, where L is the *LISA* armlength taken to be $L = 5 \times 10^9$ m. At frequencies above or near f_*, a more accurate representation of the *LISA* signal is given by the *rigid adiabatic approximation* (Rubbo et al. 2004), but detailed analysis (Vecchio & Wickham 2004) has shown that the low-frequency approximation should be adequate for most tasks at frequencies below ∼30 mHz. In this work, we have used the rigid adiabatic approximation to calculate the *LISA* signal for sources with frequencies above 0.003 Hz.

Space-borne gravitational wave observatories like *LISA* are constantly in motion, changing their relative speed and aspect with respect to astrophysical sources on the sky. The sensitivity of the observatory to different gravitational wave polarizations as a function of sky position is reflected in the antenna beam patterns, which have the highest gain in the direction perpendicular to the plane of the interferometer. As the observatory moves in its orbit, the gravitational wave signal is modulated in amplitude, frequency, and phase. Frequency (Doppler) modulation arises from the relative motion of the observatory and the source, amplitude modulation arises from the sweep of the anisotropic antenna pattern on the sky, and phase modulation results from the detector's changing response to the gravitational wave polarization state. The Michelson signal can be calculated using Equation (6) by either holding the source fixed and putting all the motion of the detector into ℓ_1 and ℓ_2 (Rubbo et al. 2004), or by holding the detector fixed and putting the motion into the source (Cutler 1998). Both approaches yield the same Michelson signal in the low-frequency limit:

$$h(t) = \frac{\sqrt{3}}{2} A(t) \cos \left[\int^t 2\pi f(t')dt' + \varphi_p(t) + \varphi_D(t) + \varphi_0 \right], \tag{7}$$

where $A(t)$ is the amplitude modulation, $f = 2/P_{\rm orb}$ (where $P_{\rm orb}$ is the binary orbital period) is the gravitational wave frequency for systems with zero eccentricity, and φ_0 is the initial phase of the wave at $t = 0$. The polarization phase, $\varphi_p(t)$, represents the phase modulation. The Doppler phase, $\varphi_D(t)$, gives the frequency modulation and the amplitude modulation is described by $A(t) = \sqrt{(A_+ F^+)^2 + (A_\times F^\times)^2}$. The sensitivity factors, F^+ and $F^\times$ are complicated functions of the position angles and orientation of the binary, as well as the position of *LISA* in its orbit (see Cutler 1998; Rubbo et al. 2004 for specific forms of these functions). The plus and cross polarization amplitudes are given by

$$A_+ = 2 \frac{G^{5/3}}{c^4 d} \mathcal{M}^{5/3} (\pi f)^{2/3} (1 + \cos^2 i), \tag{8}$$

$$A_\times = -4 \frac{G^{5/3}}{c^4 d} \mathcal{M}^{5/3} (\pi f)^{2/3} \cos i, \tag{9}$$

where d is the distance to the binary, i is the angle of inclination, and the chirp mass is $\mathcal{M} = (M_{\rm p} M_{\rm s})^{3/5} / (M_{\rm p} + M_{\rm s})^{1/5}$. We have used the approach of Rubbo et al. (2004) to calculate the timestreams, which are then added to produce the total observatory data stream, which is then Fourier transformed to produce the illustrated frequency domain representation of the double WD Galactic foreground.

The *LISA* instrument noise is simulated by assuming the power spectral density of the noise is made up of position (or shot) noise given by Cornish (2001):

$$S_{\rm np} = 4.8 \times 10^{-42} \text{ Hz}^{-1}, \tag{10}$$

and an acceleration noise (converted to strain) given by

$$S_{\rm na} = 2.3 \times 10^{-40} \left(\frac{10^{-3} \text{ Hz}}{f} \right)^4 \text{ Hz}^{-1}. \tag{11}$$

These separate components are combined according to

$$S_{\rm n} = 4 S_{\rm np} + 8 S_{\rm na} (1 + \cos^2 (f/f_*)), \tag{12}$$

Table 1
Detached Disk Double WD Formation Channels[a]

Channel[b]	Evolutionary History[c]	Rel. to Disk[d]
HeHe-D1	MT1(3-1) CE2(10-3;10-10)	8%
HeCO-D1	MT1(3-1/2/3) CE2(10-5;10-8)	6%
COCO-D1	MT1(2/3/4-1) CE2(4/7-5;7-8) MT2(7-8)	7%
COCO-D2	MT1(2/3/4-1) CE2(11-5;11-8)	3%
COCO-D3	MT1(2/3/4-1/2/3) CE2(7-5;7-8)	1%
COCO-D4	MT1(2/3-1) MT1(8/9-1) CE2(11-3;11-7) MT2(11-8)	1%
COCO-D5	MT1(3/4-1) CE2(7-3;7-7) MT2(7-8) MT1(8-11)	$\lesssim$1%
COHe-D1	CE1(6-1;11-1) CE2(11-3;11-10)	5%
The rest	$\cdots$	4%
Total	8.6×10^6	35%

Notes.
[a] GR freq. range 1×10^{-4}–0.01 Hz (5.6 hr–200 s orbital periods).
[b] In channel names XXYY, XX represents the first-formed WD.
[c] CE: common envelope phase; MT: mass-transfer (RLOF) phase. Numbers following CE or MT indicate the binary component donor star, either 1 (initially moremassive star on the zero-age MS (ZAMS)) or 2 (initially less massive star). The numbers in parenthesis correspond to the donor and accretor types; the following can be used as a guide (Belczynski et al. 2008b): 0, MS star $\leqslant$0.7 $M_\odot$; 1, MS star >0.7 $M_\odot$; 2, Hertzsprung gap; 3, red giant; 4, core helium burning; 5, early AGB; 6, thermally pulsating AGB; 7, MS naked helium star; 8, Hertzsprung gap naked helium star; 9, giant branch naked helium star; 10, helium WD; 11, carbon–oxygen WD; 12, oxygen–neon WD; 16, hydrogen WD; 17, hybrid WD. In the CE phase, the stars prior to and after the semi-colon represent the stages of evolution at the onset of and following the CE event, respectively.
[d] Percentage is relative to *LISA* binaries in said component (disk or Bulge).

where f_* is the transfer frequency. We roll off the acceleration below $f_{min} = 10^{-5}$ Hz, so that $S_{na}(f \leqslant f_{min}) = S_{na}(f_{min})$. In reality, the *LISA* noise will probably not follow this simple power law all the way down to our choice of f_{min}, but will begin to rise at a higher frequency below 0.1 mHz.

3. RESULTS

Out of our total population of compact remnant binaries with gravitational wave frequencies within the *LISA* sensitivity range, we note that $\sim$76% are double WDs, $\sim$24% are binaries involving a WD and a BD (WD–BD), while other types of binaries make up the rest (i.e., <0.5% of binaries are NS–WD binaries; less than 0.1% are NS–NS). Specific predictions for double compact objects with NSs and BHs are discussed in Belczynski et al. (2008a).

Relevant to the current study of double WDs, we find $N = 34.2 \times 10^6$ *LISA* binaries in the disk + bulge population (He, CO, ONe, and hybrid WDs)[12]. Out of this population $N_d = 24.8 \times 10^6$ (73%) and $N_b = 9.4 \times 10^6$ (27%). We find that 8.6×10^6 (25% of total) of disk binaries are detached and that 16.2×10^6 (47% of total) of disk binaries are RLOF, while for the bulge, 3.9×10^6 (12% of total) are detached and 5.4×10^6 (16% of total) are RLOF. The total number of detached binaries among the total disk + bulge *LISA* population is 12.5×10^6 (37%; 8.6×10^6 and 3.9×10^6 for the disk and bulge, respectively) while for RLOF, often neglected in previous studies, the number is 21.6×10^6 (63%; 16.2×10^6 and 5.4×10^6 in the disk and bulge, respectively). Within our RLOF population, >99% (21.4×10^6) are AM-CVn-like systems (a WD accreting from a helium or hybrid WD), the majority of which are CO WD–He WD binaries.

The number of AM CVn systems that we have found to currently exist in the MW can be compared with the estimate of Nelemans et al. (2001a). However, we remind the reader

that in our population synthesis, although we do form AM CVn stars through the helium star channel, we only include *binaries consisting of two degenerate objects* in the final results (see Nelemans et al. 2001a for a description of AM CVn formation channels). Thus, we cannot perform a direct comparison with the AM CVn population of Nelemans et al. (2001a). Nelemans et al. (2001a) find the current number of Galactic AM CVn (double WD channel only) to range between $(0.2–49) \times 10^6$, depending on the assumed effective tidal coupling (see their Section 3.4), and they find corresponding space densities of $(0.4–1.7) \times 10^{-4}$ pc^{-3}, respectively. Thus, we find that our AM CVn number estimate (21.4×10^6) is in reasonable agreement with that of Nelemans et al. (2001a) if the double WD evolutionary pathway is an efficient channel for creating these systems.

In the study of Roelofs et al. (2007b), it was determined that population synthesis studies were overestimating the space densities of AM CVn binaries, and that the true local space density is $\rho_0 = (1–3) \times 10^{-6}$ pc^{-3}, based on spectroscopic observations of six SDSS-I AM CVn stars. Adopting the disk-like density distribution as discussed in Section 2, we find that the local space density of AM CVn binaries from our population synthesis model is 2.3×10^{-5} pc^{-3},[13] which is still an order of magnitude above the most up-to-date observational estimate. It is becoming clearer that mass transfer between two WDs may not be as efficiently sustained as has been assumed in most population synthesis studies, and that a large fraction of these systems should merge upon reaching contact rather than enter the AM CVn phase (Marsh et al. 2004).

3.1. Formation Channels

We note that in our calculations, the total population of WD binaries with GR frequencies between 1×10^{-4} and 0.01 Hz comprises roughly 6% of the *total* `StarTrack` Galactic population of double WDs. While we include all RLOF double WD

---

[12] When binaries involving brown dwarfs are considered, $N = 45 \times 10^6$.

[13] For a spherical volume with a radius of 200 pc.

Table 2
RLOF Disk Double WD Formation Channels[a]

Channel	Evolutionary History	Rel. to Disk
COHe-R1	CE1(5/6-1;8/11-1) CE2(11-3;11-10) MT2(11-10)	47%
COHyb-R1	CE1(5/6-1;8/11-1) CE2(11-3;11-7/17) MT2(11-7/17)	8%
HeCO-R1	MT1(2/3-1) CE2(10-5;10-8) MT1(10-11)	5%
The rest	$\cdots$	5%
Total	16.2×10^6	65%

Note. [a] Tablenotes are the same as in Table 1.

Table 3
Detached Bulge Double WD Formation Channels[a]

Channel	Evolutionary History	Rel. to Bulge
HeHe-D1	MT1(3-1) CE2(10-3;10-10)	20%
COHe-D1	CE1(6-1;11-1) CE2(11-3;11-10)	9%
HeCO-D1	MT1(3-1/2/3) CE2(10-5;10-8)	5%
COCO-D	Various channels	3%
The rest	$\cdots$	5%
Total	3.9×10^6	42%

Note. [a] Tablenotes are the same as in Table 1.

Table 4
RLOF Bulge Double WD Formation Channels[a]

Channel	Evolutionary History	Rel. to Bulge
COHe-R1	CE1(5/6-1;8/11-1) CE2(11-3;11-10) MT2(11-10)	37%
COHe-R2	CE1(5-1;8-1) MT1(8-1) MT2(11-1/0) MT2(11-10)	20%
The rest	$\cdots$	1%
Total	5.4×10^6	58%

Note. [a] Tablenotes are the same as in Table 1.

systems that currently exist in the MW in our study, only 2.3% of Galactic detached double WD systems are accounted for, given the orbital period cutoff of ∼5.6 hr. In Tables 1–4, we show the evolutionary history (formation channels) of the most common *LISA* double WDs. We indicate the contribution (percentages) of the said channel to the population of *LISA* WD binaries from that particular Galaxy component (disk, Tables 1 and 2, or bulge, Tables 3 and 4). The characters and numbers in parentheses in the central column of the tables represent the formation channel histories, and recount various stages of stellar evolution of the primary and secondary star progenitors (see Table 1 caption for description).

In our formation channel notation, for a "CO–He" binary the CO WD is the first WD formed, but which is not necessarily the more massive WD (and thus is not necessarily the primary star). In general, the detached systems have evolved from progenitors in which the stars initially have comparable masses,[14] thus first RLOF mass transfer is more often dynamically stable and the binary does not undergo a CE at this stage (such as He–He detached double WDs). Typically, the detached double WD progenitors go through only one CE event, whereas in many cases, the RLOF binaries undergo two CE events.

We wish to point out that in the case of several RLOF binaries (e.g., those involving hybrid donors), there is a short-lived detached phase preceding the long-lived RLOF phase. For example, in the evolutionary history of a COHyb-R1 binary, the progenitor system only spends ∼10^2 Myr as a detached CO-Hyb WD after the second CE phase before being driven to contact via GR. Once contact is reached, however, the binary will spend a long time (Gyr) as a stable RLOF system. This explains why the COHyb-R1 channel shows up in Table 2, but its predecessor COHyb detached channel is absent in Table 1 (COHyb-D1 binaries only account for ∼1% of the disk formation channels for *LISA* double WDs).

In Figures 1–4, we show in (arbitrary) color the number densities of the most common formation channels for the detached and RLOF populations in the disk and bulge. We do not

include the less-populated formation channels in the plot or it would be very difficult to distinguish between channels. We do, however, include some formation channels involving BDs, since even though these binaries do not significantly affect the overall GR signal (and we have ignored them in the signal calculation), they are relatively abundant, specifically in the bulge population.

It is expected that the disk would host binaries that have evolved from a wider variety of formation channels than the bulge, since the age of the disk binaries extends over a large range: ∼few hundred Myr to 9 Gyr. Note that high-frequency systems only exist in the Galactic disk. There is a depletion of very high frequency (few minutes orbital period) RLOF systems in the bulge since the present bulge population only contains double WDs with long-lived (>9 Gyr) formation histories. All of the heavier (ONe+CO, CO+CO, and CO+hybrid) binaries originating from more massive progenitors that were born during star formation in the bulge have either long since merged, or in the case of RLOF binaries, the stars have long since reached contact and are now exchanging mass in RLOF on slowly expanding orbits.[15] Once any system encounters stable RLOF, the binary's orbital period increases as a consequence of the conservation of angular momentum under continued mass exchange, since the less massive (larger) WD is losing matter to the more massive WD. For the Galactic disk, some WD binaries are still relatively young, and are in an earlier phase of stable RLOF and thus we "catch" these mass transferring systems at shorter orbital periods (GR frequencies above ∼4.5 mHz; $P_{orb} \lesssim$ 7–8 minutes).

Typical detached evolution. Detached double CO WDs are formed through a variety of evolutionary channels. For the most prominent CO–CO channel (COCO-D1; see Table 1), one particular example of evolution proceeds as follows: two MS stars (2.88 and 2.45 $M_\odot$) start out with a P_{orb} of 14.2 days and an eccentricity of 0.54 when the MW is 9180 Myr old. At 9602 Myr, the more massive star (s1) begins to evolve off of the MS and becomes a Hertzsprung gap star. Shortly thereafter, s1 fills its Roche Lobe and begins to transfer matter to the companion (interaction between component stars aids in

---

[14] Many RLOF systems originate from systems in which the initial primary star was much more massive than the initial secondary, leading to a CE.

[15] We also note that in certain cases, particularly for bulge RLOF systems such as some AM CVn binaries, the donor has reached a lower mass limit of 0.01 $M_\odot$ at which point we no longer follow the evolution.
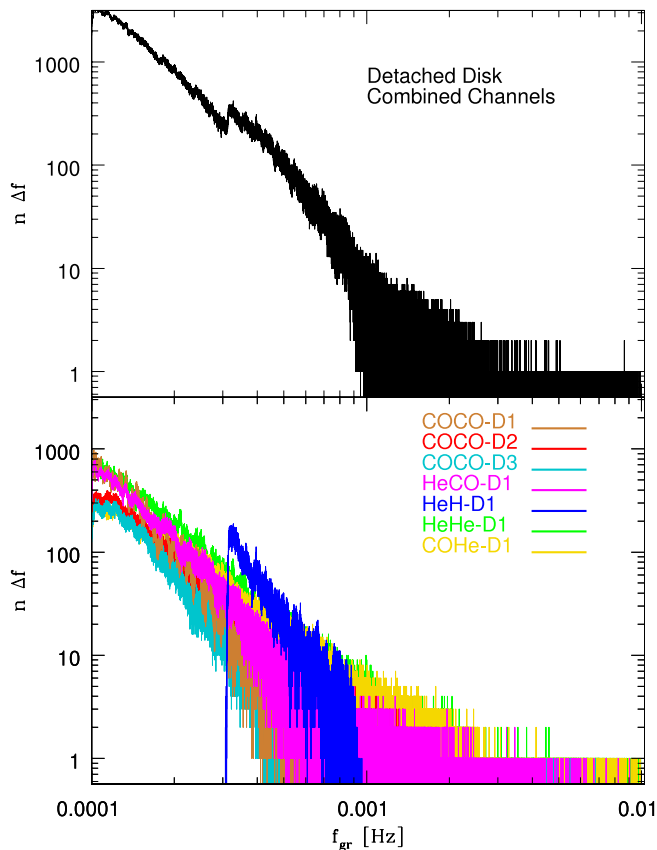
Figure 1. Number density ($n = (dN/df)$; Δf is the size of a resolvable bin for a one-year observation time, $1/T_{\rm obs} = 30$ nHz) of the most prominent detached *LISA* double WD evolutionary channels for the Galactic disk. Some channels from Table 1 have been left out for clarity, and we additionally show some of the more prominent *LISA* binary channels involving brown dwarfs (neglected in the signal calculations). Note that as the frequency increases, so does the concentration of resolvable bins.

Figure 2. Number density of the most prominent RLOF *LISA* double WD evolutionary channels for the Galactic disk. All binaries with GR frequencies $\lesssim 0.45$ mHz involve binaries with brown dwarf donors.

circularizing the orbit; $P_{\rm orb} \sim 4.5$ days). RLOF is dynamically stable, and since s1 quickly becomes the less massive star during mass transfer $P_{\rm orb}$ increases (to ~ 143 days), and RLOF stops at 9607 Myr when s1 is a red giant (0.44 $M_\odot$; core mass 0.43 $M_\odot$) and s2 (3.67 $M_\odot$) is still on the MS. s1 continues to evolve and shortly thereafter becomes a (naked) helium star (0.44 $M_\odot$), as it has lost the remaining part of its depleted (by prior RLOF) envelope. At 9731 Myr, s2 has evolved off of the MS to become a Hertzsprung gap star. By 9777 Myr, s2 has now evolved into an early asymptotic giant branch (AGB) star (3.62 $M_\odot$), and the orbital period has decreased to 81 days due to tidal interactions (expanding s2; s1 is still a helium star). s2 then fills its Roche Lobe, and since now the mass ratio is rather large ($M_{\rm don}/M_{\rm acc} \approx 8$), the mass transfer is dynamically unstable, leading to a CE phase. After the CE event the donor (s2) has become a Hertzsprung gap helium star (0.82 $M_\odot$) and $P_{\rm orb}$ has decreased by more than 2 orders of magnitude to 3 hr. The orbit then starts to decay slightly due to angular momentum losses associated with GR emission, and there is a brief RLOF phase in which the Hertzsprung gap helium star (s2) loses $\sim 0.1\,M_\odot$, half of which is gained by s1 (still a helium star, now 0.49 $M_\odot$). When the MW is 9779 Myr old, s2 finally becomes a CO WD (primary WD). s1 continues to burn helium and becomes a Hertzsprung gap helium star at 9838 Myr ($P_{\rm orb} = 2.7$ hr). Within 20 Myr, s1 then becomes a low-mass CO WD (secondary WD), finishing its helium star evolution. At 10 Gyr (present), the system is found as a detached double CO WD with component masses of 0.70
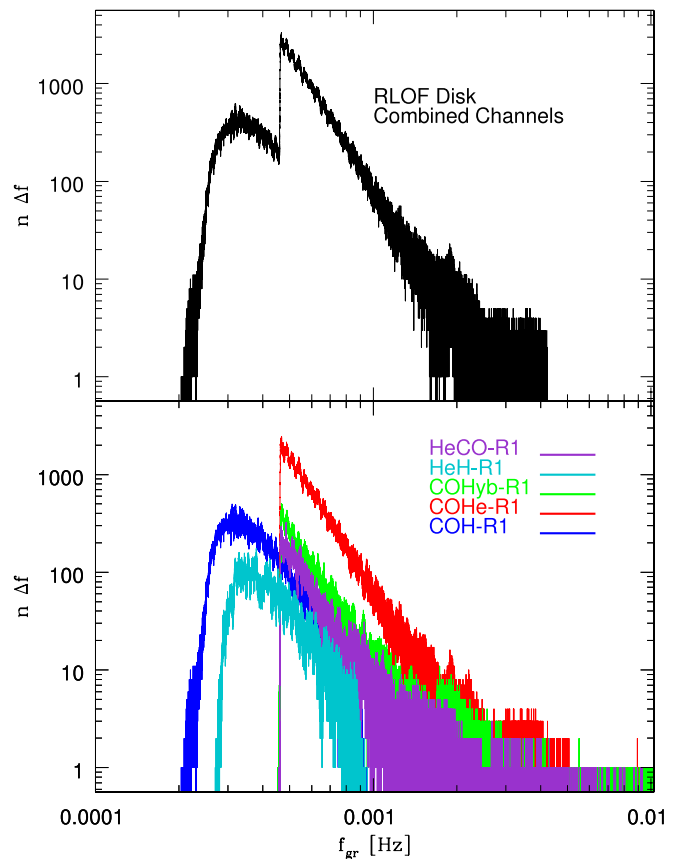
and 0.49 $M_\odot$, and $P_{\rm orb} = 2.28$ hr ($f = 0.24$ mHz). The two WDs will be brought together in ~ 300 Myr due to GR emission. The system is expected to merge due to dynamically unstable mass transfer with a combined mass of 1.19 $M_\odot$ (pre-merger orbital period of ~ 1.3 minutes). The total mass of the merged system does not exceed the canonical Chandrasekhar mass and so it is an unlikely Type Ia Supernova progenitor, though may result in the formation of a massive rapidly rotating WD (Saio & Nomoto 2004; Yoon & Langer 2005).

Typical RLOF evolution. In Figure 5, we show a representative evolution through RLOF for one of the Galactic double WDs, a COHe-R1 channel system (see Table 2). The primordial binary consists of two low-mass MS stars (2.60 and 1.40 $M_\odot$) on a wide ($P_{\rm orb} = 31.0$ yr) and eccentric ($e = 0.9$) orbit, born when the MW is 5410 Myr old. At 5966 Myr, the more massive star (s1) begins to evolve off of the MS. The orbit begins to shrink due to tidal interactions and by 6126 Myr, s1 is an early AGB star, the orbit has circularized ($e = 0$), and the period has decayed to 2.5 yr. Within 1 Myr, s1 becomes a late AGB star. Magnetic braking (convective envelope of s1) dominates angular momentum loss and the orbit decays slightly. s1 fills its Roche-Lobe (6127 Myr) and mass transfer is unstable, leading to a CE phase and a drastic decrease in orbital period (from 2.4 yr to 8.2 days). s1 then becomes a CO WD (primary WD, 0.64 $M_\odot$). At 8782 Myr, s2 evolves off of the MS. The orbit decays due to magnetic braking (convective s2), and at 9085 Myr, s2 initiates a CE phase resulting in another prominent period decrease (6.1 days to 30 minutes) and the loss of its hydrogen-rich envelope. s2 then becomes an He WD (0.22 $M_\odot$). GR causes the WDs to come into contact a few Myr later ($P_{\rm orb} \sim 3$ minutes),
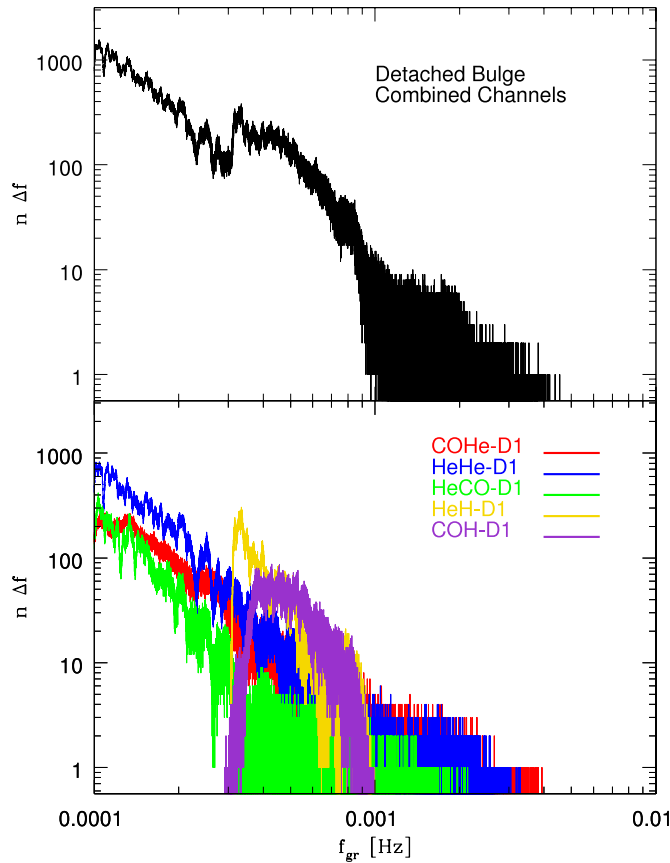
Figure 3. Number density of the most prominent detached *LISA* double WD evolutionary channels for the Galactic bulge.
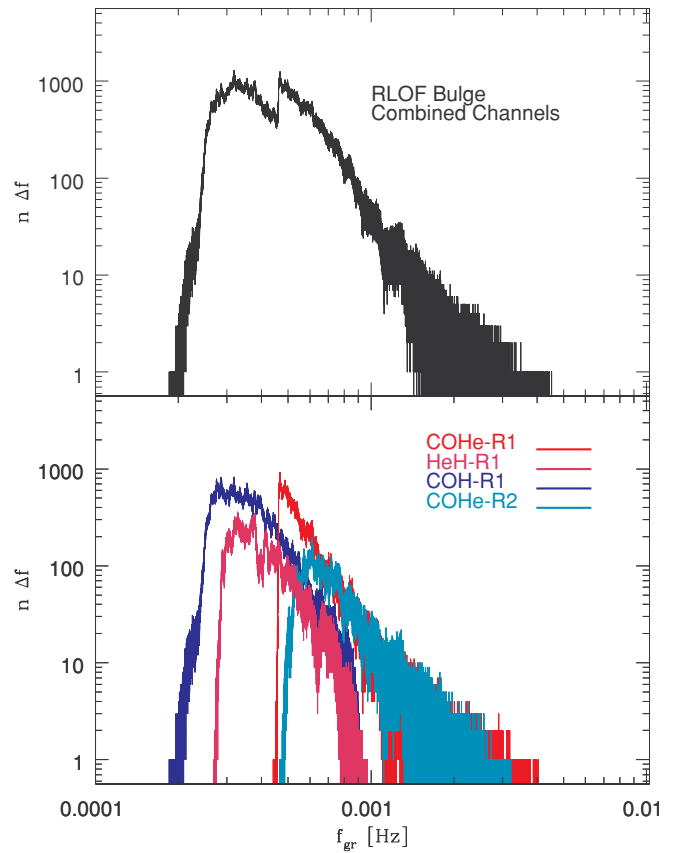

Figure 4. Number density of the most prominent RLOF *LISA* double WD evolutionary channels for the Galactic bulge. Note that COHe-R1 is descended from COHe-D1 in Figure 3, in which the binary undergoes two CE phases.

and the secondary (s2) fills its Roche Lobe. The mass ratio is only ~0.34, thus RLOF is stable, and an AM CVn system is born. Initially, mass transfer is quite rapid (see Figure 5, top panel), but a slower mass-transfer phase follows. The binary is found at 10 Gyr with $P_{orb} \sim$ 1 hr (~0.6 mHz) and with component masses of 0.83 and ~0.01 $M_\odot$ for the CO and He WDs, respectively. Many of the 25 observed AM CVn binaries' parameters are uncertain, and detection of these systems is biased against the typical, longer-period systems with lower mass-transfer rates. However, this particular simulated binary's properties are somewhat similar to the very few long-period AM CVn binaries that have been detected (e.g., SDSS J1552 and CE 315), though the nature of the donors is still unknown (Anderson et al. 2005; Roelofs et al. 2007b).

3.2. Detached Population Characteristics

Characteristic properties of the entire detached population are shown in Figure 6. Disk systems are found at all orbital periods (top panel) within the *LISA* sensitivity range, with a drop in number at shorter periods due to the fact that once systems reach contact, double WDs either fall into the RLOF population or otherwise merge and drop out of the *LISA* population altogether. The masses of the secondaries (M_s, less massive WDs, middle panel) lie predominantly in four regions: ~0.1 $M_\odot$ (He WDs with CO primaries), a prominent peak near 0.3 $M_\odot$ (mostly He with some hybrid WDs with mostly CO or He companions), a small clump near 0.5 $M_\odot$ (CO secondaries with CO primaries), and a short peak at ~0.7 $M_\odot$ (CO or sometimes ONe secondaries with either CO or ONe primaries). The He secondaries with very low mass (0.1 $M_\odot$) derive from the same formation channels as

cataclysmic variables (similar systems have been discussed in Podsiadlowski 2008), in which a CO WD accretes from a low-mass MS star for several Gyr (note the higher number of these systems in the Galactic bulge). Eventually, the donor becomes fairly exhausted of its hydrogen supply, and meanwhile has built up a significant helium core. The donor is eventually depleted of so much mass that it reaches the hydrogen burning limit (0.08 $M_\odot$), and thus becomes degenerate (in this case, helium rich—a helium WD). Many of the systems whose secondary mass peaks near 0.3 $M_\odot$ are progenitors of AM CVn stars (COHe), while most of the binaries involving more massive progenitors (CO and ONe) will likely merge once they reach contact. Primary WDs (M_p, more massive WDs; bottom panel) display a peak at 0.3–0.4 $M_\odot$, though most primaries have masses 0.5–0.8 $M_\odot$, and a smaller number of systems are quite heavy (0.8–1.4 $M_\odot$). The low-mass peak is comprised of He WD primaries, with He secondaries. The majority of the rest are CO WDs, with either He or CO secondary companions. In both the middle and bottom panels, we note that there are relatively fewer heavy WDs in the bulge population. This is because all of the more massive progenitors (e.g., CO–CO) have had a sufficiently long enough time to evolve off of the MS, encounter 1 or 2 CE phases, reach contact (GR is also more efficient at bringing together two CO WDs than two He WDs) and have either merged out of the population altogether or in some cases, have moved into the RLOF population. A two-dimensional gray-shaded plot is presented in Figure 7, where we show the relationship between the secondary and primary masses of *LISA* binaries in the Galactic disk, presented in terms of relative total percentages of *LISA* double WDs.
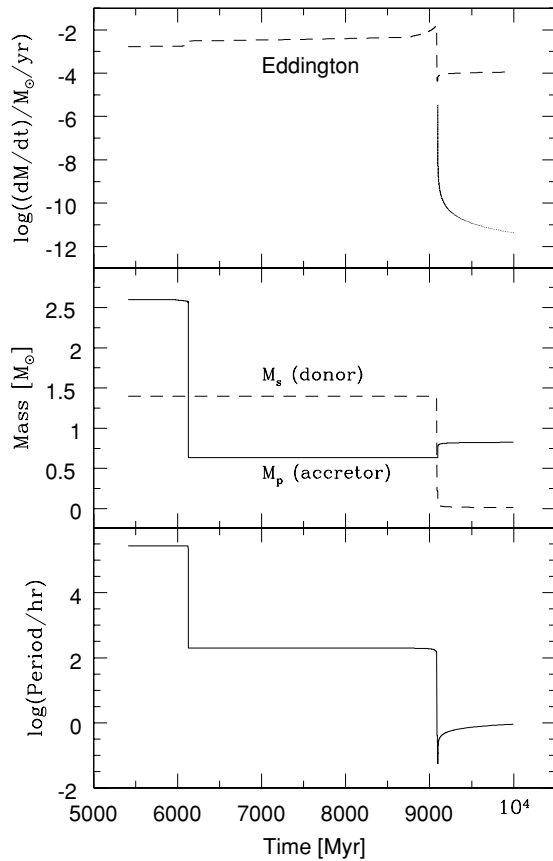
Figure 5. Characteristic evolution as described in Section 3.1 of an RLOF system with a CO WD accretor and an He WD donor, from the AM CVn formation channel COHe-R1 starting at the ZAMS. Top panel shows the mass-transfer rate evolution (with the critical Eddington rate shown), middle panel shows the mass change of the two components, while the bottom panel illustrates the orbital period evolution. The two CE phases coincide with the prominent drops in orbital period when the donor (initial primary) is a late AGB star, and then when the donor (initial secondary) is a red giant. Stable RLOF begins at the period minimum of ∼3 minutes, when the Galaxy is 9.1 Gyr old.

3.3. RLOF Population Characteristics

Characteristic properties of the entire RLOF population are shown in Figure 8. The RLOF systems with the maximum P_{orb} (lowest GR frequencies) appear at ∼75 minutes ($\log(f_{gr})$= −3.34). The shape of the period distribution (top panel) is due to the fact that most systems spend the majority of their time at periods of ∼1 hr during the dynamically stable RLOF phase. As indicated previously, 99% of RLOF systems are AM CVn (a WD accreting from an He or hybrid WD). For most WD binaries, at the onset of stable RLOF, orbital periods are on the order of only a few minutes, and mass-transfer rates are initially high (see Figure 5, top panel). The donor quickly becomes exhausted of most of its mass, the mass-transfer rate decreases, and the period continues to increase, though at a much slower rate. In the middle panel, we show WD secondary masses, which are strongly peaked at ∼0.01 $M_\odot$, with a slight drop-off to 0.045 $M_\odot$. These WDs are comprised of mostly He WDs, some hybrid WDs and a small number of CO WDs. The "pile-up" of WDs at 0.01 $M_\odot$ stems from the fact that once an AM CVn WD–WD progenitor reaches contact, the mass-transfer rates are initially high (∼10^{-6} $M_\odot$ yr^{-1}) and the donor is rapidly exhausted of mass, and thus it is rare to catch AM CVn secondaries that are relatively massive (>0.02 $M_\odot$). In the bottom panel, we show the distribution of masses among the primary WDs, which are
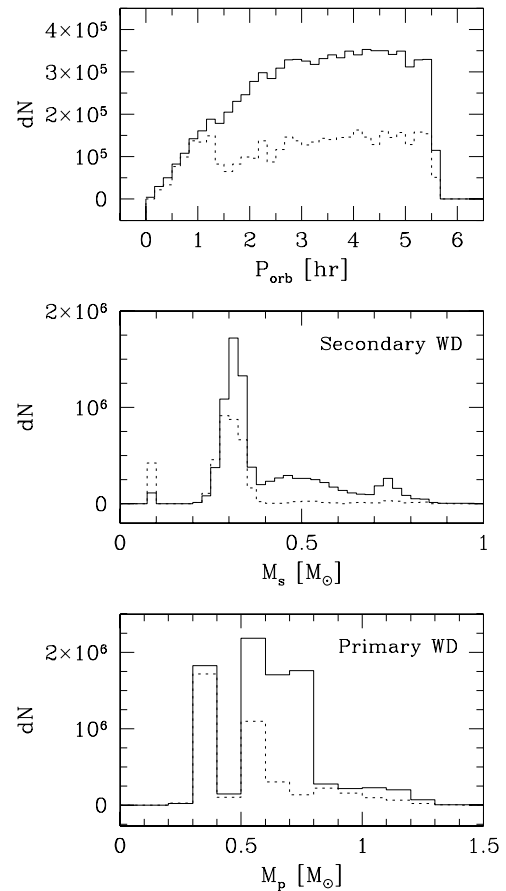

Figure 6. Physical properties of the Galactic population of detached *LISA* double WDs. The solid line shows the disk binaries, whereas the dotted line shows the contribution from the bulge. Bottom and middle panels show the distribution of primary and secondary mass (more massive and less massive WD, respectively), while the top panel shows the orbital period distribution. Note the different bin size and scales used on the axes.
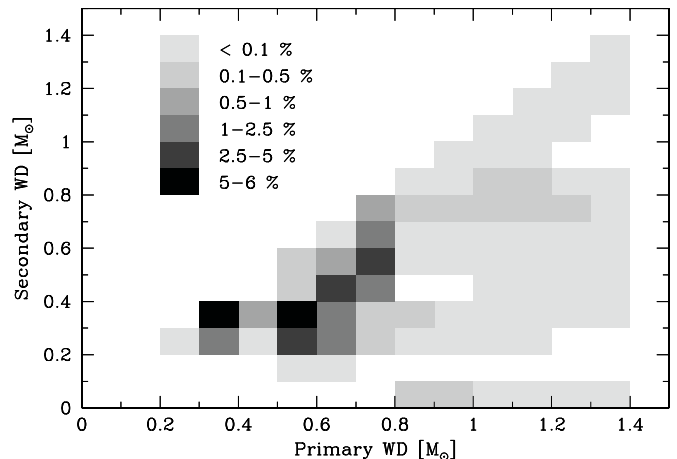

Figure 7. Primary and secondary WD masses for Galactic disk detached *LISA* binaries (corresponding to the solid line histogram in Figure 6). The gray scale shows the relative contributions (percentage wise) relative to the Galactic disk *LISA* double WD population.

mostly CO WDs, with a small contribution of ONe WDs (masses >1.3 $M_\odot$). We show in Figure 9 a two-dimensional gray-shaded plot of RLOF *LISA* binaries in the Galactic disk, presented in terms of relative total percentages of *LISA* double WDs.
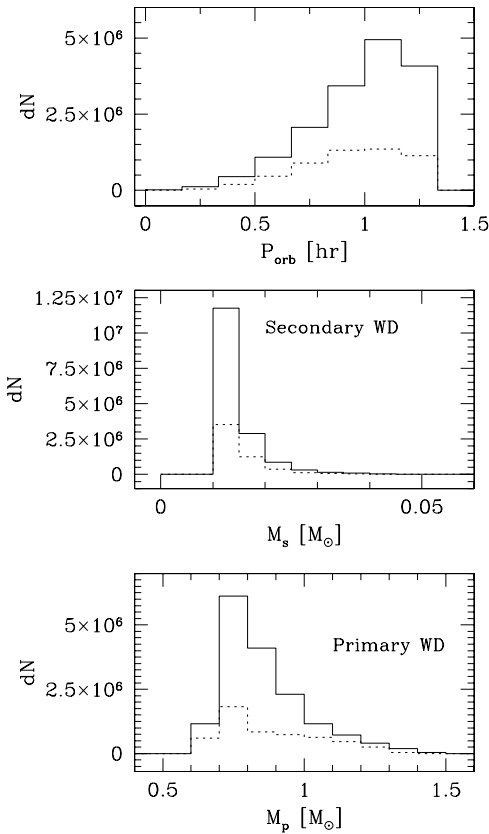
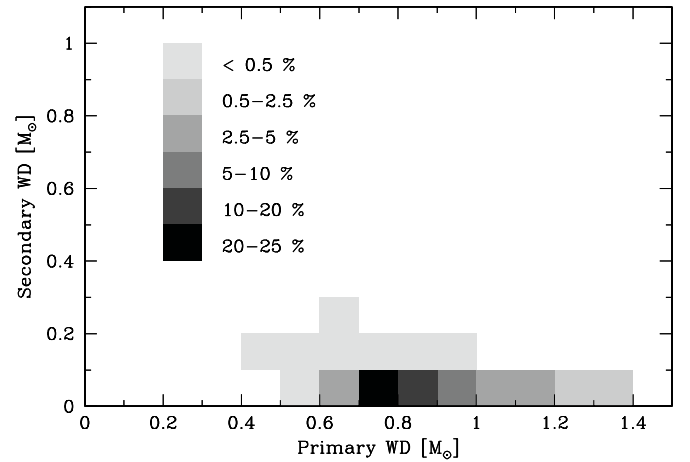**Figure 8.** Same as Figure 6 but for RLOF systems.

Figure 9. Primary and secondary WD masses for Galactic disk RLOF *LISA* binaries (corresponding to the solid line histogram in Figure 8). The gray scale shows the relative contributions (percentage wise). Note the different scaling on the *y*-axis as compared to Figure 7.

4. *LISA* SIGNAL

During a one-year observation period, the width of a resolvable frequency bin is $\Delta f = 1\,\mathrm{yr}^{-1} \approx 3 \times 10^{-8}$ Hz. Below 1 mHz, there are hundreds to thousands of binaries per resolvable frequency bin, causing the signal to be confusion limited. In our simulation, below $\sim$0.45 mHz, the only contributing binaries to the *LISA* signal are the detached double WDs.

The *LISA* spectra (amplitude densities, or spectral amplitudes h_f) for the Galactic double WDs were calculated using the sophisticated *LISA* simulator of Benacquista et al. (2004), and are shown in Figure 10. Close binaries that evolve to contact, such as the precursors to the AM CVn population or progenitors of WD mergers, will spend a very short time (<1 Myr) at GR frequencies >0.01 Hz ($P_\mathrm{orb} \lesssim 3$ minutes, provided they reach these short periods), and this is reflected in our orignal `StarTrack` calculations. Thus, we artificially truncate the signal above 0.01 Hz since we simply do not have a large enough number of `StarTrack` binaries above this frequency in order to accurately extrapolate them to the total number of Galactic systems here. However, we expect the number of *LISA* systems above 0.01 Hz to be $\lesssim 10^3$. In the bottom panel, we show the spectra from the four Galactic sub-populations, while in the top panel we show the full spectra for the combined population (gray) with a running median over 1000 frequency bins (white). The white curve represents our Galactic double WD foreground (see Section 4.2). We also show the foreground estimates of Nelemans et al. (2004; dotted pink) and Hils & Bender (2000; dashed orange) for comparison. The foreground of Nelemans et al. (2004) was artificially truncated beyond $\sim$2 mHz, above which individual binaries were expected to be resolvable in that work. It is immediately noticed that the bulge binaries (green

and mauve; lower panel) do not contribute to the GR signal above $\log(f_\mathrm{gr}) = -2.35$ ($f_\mathrm{gr} = 4.5$ mHz) for reasons discussed in Section 3.1. Also, the RLOF binaries do not contribute to the signal at low frequencies (below $\log(f_\mathrm{gr}) = -3.34$, $f_\mathrm{gr} = 0.45$ mHz) since these are binaries that have been in a state of RLOF for a prolonged period of time, and are on very slowly expanding orbits (largest orbital period $\sim$75 minutes). Additionally, once the donor mass drops below 0.01 $M_\odot$, we stop the calculation; thus, these very low mass, low frequency systems do not contribute to the calculated *LISA* signal.

The RLOF disk signal (blue; lower panel) becomes comparable to the detached disk signal (red; lower panel) at frequencies above $\sim\log(f_\mathrm{gr}) = -2.5$ ($f_\mathrm{gr} \sim 3$ mHz). In our calculations, the AM CVn binaries spend only a short period of time ($\sim 10^1$–10^2 Myr) as detached double WDs, where as they may spend $\sim$Gyr in the RLOF phase. This is likely a consequence of the CE prescription that we have employed, and most AM CVn systems go through a double CE (COHe-R1 channel). The Webbink (1984) CE prescription with $\alpha \times \lambda = 1$ produces relatively close post-CE WDs, and so it does not take long for the stars to be brought into contact via GR once the detached double WD has been formed.

In the upper panel, we show our combined signal (gray) and the median foreground (white line) alongside the astrophysical foreground estimates of Hils & Bender (2000) and Nelemans et al. (2004), both of which include detached and AM CVn binaries. Note that our foreground is significantly lower than the classic Hils & Bender (2000) estimate at low frequencies, and is more comparable to the curve of Nelemans et al. (2004) in this regime (see below). Our foreground curve has been smoothed over 1000 bins, but some "bumpiness" still exists at higher frequencies due to low number statistics. In contrast to some previous studies where the signal has been truncated at higher frequencies, we show the curve over a significant portion of the *LISA* bandwidth, up to 0.01 Hz. Since our original `StarTrack` binary population was scarcely populated at high frequencies, consequentially we could not generate smooth formation channel PDFs (Section 2.2) for high-frequency systems.

Our level of foreground signal is below that of Nelemans et al. (2004) for GR frequencies $\lesssim$0.0013 Hz. This is in part due to the fact that at low frequencies, there is an overall lack of *LISA*
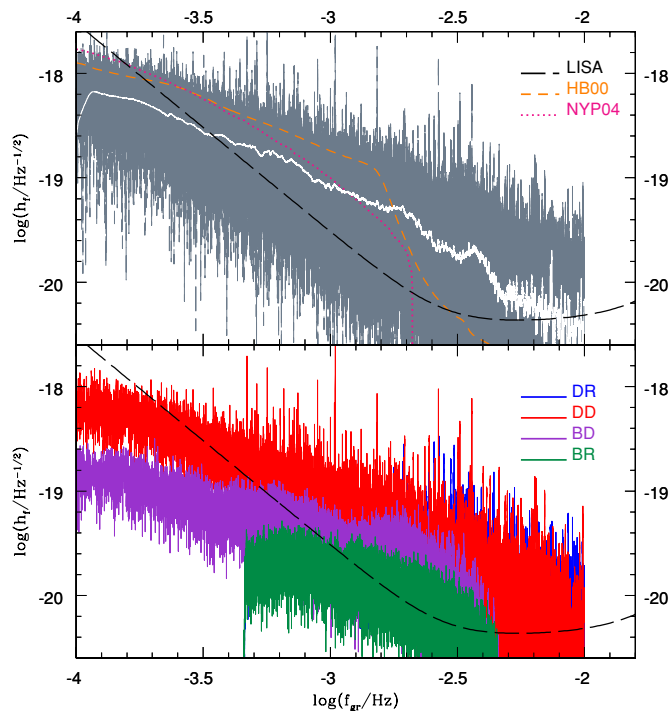
Figure 10. Spectra (amplitude density) of the gravitational wave signal for *LISA* galactic WD binaries. Bottom panel: disk detached (red), bulge detached (mauve), disk RLOF (blue), and bulge RLOF (green). Top panel: the combined population is shown with no smoothing (gray), and with a running median over 1000 bins (white). Additionally, the foreground estimates of Nelemans et al. (2004; dotted pink) and Hils & Bender (2000; dashed orange) are shown for comparison. Both panels: note that the signals have been truncated at frequencies above 0.01 Hz (see the text). The standard *LISA* sensitivity curve (black long dash) for a signal-to-noise ratio of 1 is also shown.

binaries, since a large fraction of our *LISA* binary population are RLOF systems and hence do not exist at the low end of the frequency spectrum.[16] The median chirp mass of our double WDs at frequencies below ~ 0.0013 Hz is $\sim 0.38\,M_{\odot}$ (disk) and $0.31\,M_{\odot}$ (bulge).

Despite the large number of RLOF systems in the low-frequency, confusion-limited region of the Galactic gravitational wave spectrum (Figures 2 and 4), the amplitude of the gravitational wave signal at low frequencies is dominated by the detached double WDs. Mass-transferring binaries at lower frequencies have undergone a significant amount of mass transfer, which leaves them with lower chirp masses than the detached binaries. As discussed previously, RLOF systems do not occur with orbital periods greater than ~ 1.5 hr ($f_{\rm gr} \lesssim 0.45$ mHz). Consequently, the gravitational wave amplitude of the RLOF systems (both from the disk and from the bulge) does not contribute very strongly to the overall foreground noise in the low-frequency regime. The GR amplitude from the bulge is smaller than that of the disk for both (corresponding) detached and RLOF components of the disk, primarily due to the fact that the stellar mass of the bulge is $\sim 1/3$ the mass of the disk, and contains fewer *LISA* double WDs.

4.1. Transition Frequency

The "transition frequency" is said to correspond to the GR frequency at which the gravitational wave spectrum transitions from confusion limited to individually resolvable sources. The

exact conditions that are necessary in order for this to occur (one possibility would be when the average number of binaries per frequency bin drops below 1 are not completely clear. The addition of RLOF systems to the detached population will increase the frequency at which the average number of binaries per bin drops below 1 simply by adding more sources to the population. This is particularly so since RLOF binaries are able to maintain short orbital periods (for longer than their detached counterparts) once contact has been established. Furthermore, as the transition frequency increases, the spread of the signal due to the motion of *LISA* also increases, thus the signals will continue to overlap at higher frequencies than might be inferred from a simple analysis of the number of binaries per resolvable frequency bin. For a simple detached system in a circular orbit whose orbital period is evolving solely due to the emission of GR, seven parameters are needed to fully characterize the signal. Basic estimates from information theory describe how the limited amount of information in the *LISA* data stream can be mapped onto an equivalent amount of information about detected binary systems. A common rule of thumb is the "three-bin rule": at least three (otherwise unpopulated) frequency bins of *LISA* data are needed to resolve a seven-parameter binary source (see Timpano et al. 2006 and references therein for a discussion). One can reasonably expect that a mass-transferring system will require more parameters to characterize the GR signal, and consequently more frequency bins to individually resolve the source. Therefore, the average number of binaries per frequency bin is not a particularly good indicator of how the transition frequency changes with the addition of the RLOF population.

For the sake of comparison with previous studies, we have estimated the transition frequency using the three-bin rule method. The point at which *LISA* binaries *start* to occupy one source per three frequency bins is found to be 1.5 mHz for the detached *LISA* binaries only, which is comparable to Nelemans et al. (2001b) and Nelemans (2003b), who found a transition frequency of 1.5–2 mHz (see also Nelemans et al. 2004 for a discussion of the inclusion of AM CVn binaries in the confusion limit calculation). However, we find that when we consider the entire *LISA* population of double WDs, the transition frequency is increased to 2.4 mHz. We would like to point out however that these frequencies do not represent the frequencies above which one expects to resolve all *LISA* binaries; there are still a number of populated bins at higher frequencies.

The three-bin rule method of estimating the frequency at which binaries start to become resolved is not a robust method, since it is expected that at these higher frequencies, the frequency evolution due to mass-transferring binaries can contribute a significant additional spreading of the signal. Further, this method does not take into account important criteria such as Doppler, phase, and amplitude modulation, and one should consider alternative (more technical) methods in computing the transition frequency region (e.g., chapter 2 of Ruiter 2009). In the following subsection, we discuss an approach other than the three-bin rule of thumb to identify the population of resolved sources. Instead of using a general estimator like the transition frequency, it is possible to use a predicted signal-to-noise ratio (S/N) for any particular system to determine whether it is potentially resolvable or not (see also Timpano et al. 2006).

---

[16] We wish to point out that the number of binaries per resolvable frequency bin at 0.0001 Hz in Nelemans et al. (2001) is a factor of ~ 2 higher than ours.

4.2. Noise

For *LISA* observations of length T_{obs}, the sensitivity to a particular binary source can be expressed by constructing a simple estimator of the S/N. For circularized compact binaries, long observations will narrow the bandwidth of the source, and the binary will appear in the Fourier spectrum as a narrow spectral feature with root spectral density $h_b(f)$, given in terms of the strain amplitude h_o as (Larson et al. 2000)

$$h_b(f) = h_o \sqrt{T_{obs}}. \tag{13}$$

LISA will detect binaries in the presence of competing sources of noise. There will be two components to the noise in *LISA* analysis: instrumental noise in the detector itself and irreducible astrophysical noise from the total population of Galactic close binaries. The instrumental component of the noise is given by the shape of the *LISA* sensitivity curve (Larson et al. 2000). In this work, the Galactic foreground noise is computed from the synthesized Galaxy itself (i.e., with `StarTrack`). The gravitational wave strength of every binary in the synthesized Galaxy is estimated from its parameters, and a running median of the total signal is computed as a function of frequency. Since the total number of individually resolved binaries is expected to be small compared to the total population, the running median should be a good estimate of the residual astrophysical noise foreground that would result from a fully realized science analysis procedure. The foreground resulting from this procedure has been shown in Figure 10 (top panel). Additionally, we have calculated the median foreground signal that is expected to arise from the unresolvable sources alone (the "Reduced Galaxy"), which is likely a more realistic estimate of the true Galactic foreground. In Figure 11, we show the Galactic foreground alongside the Galactic foreground signal minus the signal arising from the sources that were determined to be resolvable using our signal-to-noise estimate technique, assuming an S/N > 5 (see Section 4.3). Alongside our Galactic foregrounds, we show for comparison the standard *LISA* sensitivity curve as well as the average Michelson noise of *LISA*. The latter curve (see Section 2.3) is a more appropriate comparison of the *LISA* instrumental noise with our calculated gravitational wave signal from the Galactic binaries, as both curves (our signal and the Michelson noise) account for directional and frequency dependencies of the wave as measured by *LISA* (Rubbo et al. 2004). The standard *LISA* sensitivity curve (Larson 2000) is often presented in the literature, and is an approximation of the spectral amplitude h_f scaled from the barycenterd sensitivity amplitude h_o from the *Online Sensitivity Curve Generator*.

The ultimate level of the confusion foreground (and as a result, the ultimate S/N of any given source) will depend strongly on the actual data analysis algorithm used to identify and subtract sources. To date, no fully realized implementation of such a procedure has been developed. The computed foreground shown here should be a good estimate of the output of a fully developed analysis procedure.

4.3. Resolvable Sources

Though millions of double WDs are expected to be detected with *LISA*, a much smaller number of these systems are predicted to be resolved, depending upon the physical properties of each binary (see also Stroeer et al. 2005 for a discussion). Due to the small separations of these compact binaries, Cooray et al. (2004) predicted that nearly 1/3 of the resolved *LISA* binaries will be
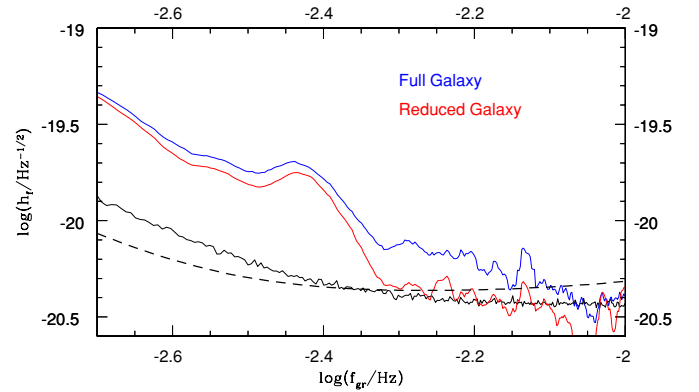

Figure 11. Median signal shown in Figure 10 (smoothed): the median Full Galaxy (upper-most curve, blue) alongside the median Reduced Galaxy (lying just below Full Galaxy; full median signal with resolved sources removed, red), the standard *LISA* sensitivity curve (dashed line; S/N = 1, also shown in Figure 10), and the simulated *LISA* Michelson noise curve (Section 2.3). As in Figure 10, the spectra have been truncated above 0.01 Hz. Both the Full Galaxy *LISA* double white dwarf foreground (blue line) and the Reduced Galaxy foreground curve (red) fall below the Michelson noise at roughly ∼8 mHz, where the curves are relatively noisy. When one considers the median foreground spectra against the standard sensitivity curve, the Full Galaxy foreground drops below the sensitivity curve at ∼7.5 mHz, while the Reduced Galaxy foreground drops below the sensitivity curve at ∼6 mHz. The (black) noise curves differ in sensitivity level and shape since the underlying noise levels used to generate each noise curve are different. In our study, we have used the Michelson noise curve to represent the *LISA* instrumental noise; the standard sensitivity curve is shown for comparison.

(A color version of this figure is available in the online journal.)

eclipsing in the optical regime and thus will offer an opportunity for these systems to be studied with follow-up observations, allowing for the determination of WD physical parameters (i.e., radii). It has been noted by Nelemans (2009), however, that the intrinsic brightness of WDs was overestimated in Cooray et al. (2004), and thus the expected number of *LISA* double WDs with electromagnetic counterparts should be lower. Nelemans (2009) predict a smaller, though still relatively optimistic, number of *LISA* systems that may have optical and/or near infrared counterparts—possibly as many as ∼2000 sources (see their Section 3.3).

The total effective noise in the detector (instrumental + foreground) is given by the spectral amplitude $h_f(f)$, and the S/N is estimated as (Larson et al. 2000)

$$S/N \simeq \frac{h_b(f)}{h_f(f)} = \frac{h_o \sqrt{T_{obs}}}{h_f(f)}. \tag{14}$$

A binary is deemed "resolvable" (distinguishable from the confusion limited Galactic foreground) if its S/N is greater than some detection threshold (typical S/N ⩾ 5). Additionally, resolved sources in the population are sorted into *monochromatic sources* and *chirping sources*. Monochromatic sources do not evolve appreciably over the *LISA* observing time, T_{obs}. A binary is considered to be chirping if its frequency changes by more than the *LISA* frequency resolution, $\Delta f \geqslant 1/T_{obs}$. This criterion is a conservative one, as the expectation is that *LISA* will be able to detect frequency changes that are smaller than the frequency resolution Δf (Takahashi & Seto 2002). The detection of binaries with appreciable evolution in f (or "chirp") is useful, since this frequency evolution allows for the determination of $\mathcal{M}$, from which the distance to the source can be calculated (see, e.g., Nelemans et al. 2001b).

The estimate of the S/N in Equation (14) will not be precise in the regime where orbital periods change on timescales that are short compared to the observation time, or where the shape of the instrumental noise changes appreciably as a function of frequency. However, this simple estimator is a good tool to use as a first cut in a search over a large population of sources where a calculation of the S/N for each binary would be computationally prohibitive. For the purposes of this paper, this estimator should be perfectly adequate since in large part the binaries of interest are not chirping across a significant portion of the *LISA* band during T_{obs}. Once a set of Galactic binaries has been identified using the simple estimator in Equation (14), it is computationally plausible to consider a more robust estimate of the S/N for each system, which can then be constructed from the data analysis technique of choice. For example, with chirping binaries a good estimate of the S/N can be motivated from matched filtering techniques by integrating over a binary's spectral energy distribution, dE/df (Flanagan & Hughes 1998).

Using this simple S/N estimator to resolve *LISA* binaries, we find that a total of $\sim$11,300 double WDs will be resolvable in our Galactic sample: $\sim$600 chirping and $\sim$10,700 monochromatic. This is inferred under an optimistic assumption that all binaries with an S/N > 5 have a chance to be resolved. Within the resolvable population, we find $\sim$4000 AM CVn binaries and $\sim$500 possible double degenerate scenario—DDS; Iben & Tutukov (1984); Webbink (1984)—SN Ia progenitors (detached COCO WD binaries that will merge within a Hubble time, whose total mass exceeds the Chandrasekhar mass limit). Out of these possible SN Ia progenitors, the majority are formed through the COCO-D4 channel, which involves the most massive primaries on the ZAMS. As for the AM CVn resolvable binaries, 7% are chirping and arise mostly from COHe-R1 and COHyb-R1 channels, in near-equal numbers. Both formation channels involve two CE events and thus if these systems will be resolved with *LISA*, they will serve as useful objects for understanding close binary evolution. Additionally, a number of progenitor AM CVn binaries are resolvable ($\sim$3000; detached channels), but only $\sim$100 of these are chirping.

If we relax our criteria and assume that any binary with an S/N > 1 is potentially resolvable, we find $\sim$43,000 resolvable double WDs ($\sim$1000 chirping and $\sim$42,000 monochromatic). Additionally, we find $\sim$2800 *LISA* binaries with S/N > 10, $\sim$300 of which are chirping sources. The binaries with large S/N ($\gtrsim$10) typically all have orbital periods $<$2000 s ($f_{gr} >$ 0.001 Hz) and have either just recently encountered RLOF, and thus they still have relatively large chirp masses, or they are close to reaching contact.

In Table 5, we show a breakdown of the 11,300 (2800) potentially resolvable *LISA* double WDs that have S/N > 5 (S/N > 10), with percentages relative to the resolvable population in question. The properties of those resolved systems reflect some of the selection effects that are expected to arise from using *LISA* to identify double WDs. Systems with short orbital periods (and consequently high gravitational wave frequencies) are favored both because the amplitude of the signal scales as $f^{2/3}$ and because the number of binaries per bin drops with increasing frequency. Furthermore, systems with large chirp masses are favored simply because the amplitude of their GR scales as $\mathcal{M}^{5/3}$. Thus, we see that the resolvable population is biased toward high-mass, high-frequency (short period) systems. Realistically speaking, it is still unclear as to which method(s) of detecting resolvable binaries with *LISA* will be most successful,

Table 5
Expected Number of Resolvable *LISA* Double WDs

Type[a]	% S/N > 10	% S/N > 5
Detached		
HeHe-D1	8.4	9.4
HeCO-D1	6.3	5.5
COCO-D1	1.2	1.8
COCO-D2	3.6	3.2
COCO-D3	2.3	1.8
COCO-D4	9.1	5.3
COCO-D5	1.4	1.4
COHe-D1	23.0	22.3
COHe-D2	0	<1
COHyb-D1	1.2	1.2
The rest	< 1	<1
Total	57.0	53.0
RLOF		
COHe-R1	17.3	21.4
COCO-R1	10.2	11.0
COHyb-R1	9.9	8.4
HeCO-R1	2.6	2.6
HeHe-R1	1.6	1.9
HybCO-R1	1.2	1.5
The rest	< 1	<1
Total	43.0	47.0
Total	2800	11300

Notes. Formation channels producing resolvable *LISA* double WDs in the Galaxy, assuming that every binary with S/N $\geqslant$ 10 or S/N $\geqslant$ 5 with a gravitational wave frequency below 0.01 Hz has a chance to be resolved. Relative percentages (with respect to the total resolved population for the appropriate S/N threshold) for each channel are indicated.

and so we have discussed the likelihood of potentially resolving individual binaries using a few different methods.

Detached resolved sources. A large number of the resolved sources are of the HeHe-D1 channel, where two initially low-mass ($\sim$1 $M_\odot$) evolved stars lose their envelopes during mass-transfer phases. HeHe-D1 is not only the most prolific formation channel of detached systems (Tables 1 and 3), but it also extends to high GR frequencies. Lumping all of the COCO-D formation channels together, COCO detached binaries make up $\sim$13%–18% of the resolved population, and potential DDS progenitors make up 5% of the total resolved population. Though HeCO-D1 double WDs are more numerous compared to COHe-D1 binaries, fewer of them are resolved. We note that COHe-D1 progenitors involve two CE phases (HeCO-D1 only one), and overall occupy closer orbits thus contributing to higher GR frequencies.

RLOF resolved sources. For RLOF systems, the majority are of AM CVn type. The most common RLOF channel is COHe-R1, followed by COCO-R1. COCO-R1 binaries are not common, but they lie on very close orbits, consisting of a massive ($\sim$1 $M_\odot$) CO WD accreting matter from a low-mass ($<$0.2 $M_\odot$) CO WD. The resolved COHe-R1 AM CVn systems account for most of the total number of resolved AM CVn binaries. Since the formation of these systems involves two CE events, future *LISA* observations may put some very useful constraints on this rather uncertain evolutionary phase, which is crucial to the formation of close binaries. However, when comparing relative formation scenarios of AM CVn binaries, we must keep in mind that the precise behavior of the stars upon reaching contact—and the exact physical conditions of the donor at contact—are still unclear, as are the physical characteristics of the AM CVn progenitors

themselves. Further observations and detailed modeling will be an important step toward understanding the donors in AM-CVn-type systems (Deloye et al. 2007). For example, deviations from the equilibrium evolution of AM CVn systems, e.g., brought on upon by changes in the mass-transfer rate following a nova explosion, result in a measurable frequency evolution, which can greatly differ from what is expected for the long-term, equilibrium evolution case. This was already shown by Stroeer & Nelemans (2009); if short-term changes in the evolution of AM CVn systems are neglected, it can lead to erroneous estimations of some of the binary parameters.

5. COMPARISON WITH PREVIOUS STUDIES

The number of binaries that are important in the context of the *LISA* GR signal was estimated by Hils et al. (1990), and in their work they predicted 3×10^7 Galactic close double WDs (orbital periods $\lesssim 1$ day) based upon a surface density star formation rate. However, that estimate seemed to overpredict the observed local density of double WDs available at that time. They concluded that even if they decreased the estimated space density by a factor of 10 (decreasing the total number of Galactic double WDs), close WD binaries would continue to dominate the *LISA* GR signal at low frequencies (Hils et al. 1990, Section 1). Population synthesis studies (e.g., Nelemans et al. 2001) which incorporate current estimates of Galactic star formation rates and SNe rates result in a higher number of Galactic double WDs ($\gtrsim 21 \times 10^7$),[17] albeit the majority of these would have orbital periods too large to be detectable with *LISA*. Still, we note here that current estimates of the number of double WDs with GR frequencies detectable with *LISA* are a factor of ~ 10 higher than those used in 1990.

To populate the Galaxy (the disk only), Hils et al. (1990) used the density distribution

$$\rho = \rho_0 e^{-R/R_0} e^{-|z|/z_0}, \tag{15}$$

where ρ_0 is the central density, R and z are galactocentric cylindrical coordinates, and R_0 and z_0 are the radial scale length and vertical scale height of the Galactic disk, respectively. Hils et al. (1990) used $z_0 = 90$ pc in their study, and while it is a reasonable assumption for the scale height of the thin disk, this likely led to their (too) low estimate of double WDs. More recently, it has been noted (e.g., Benacquista & Holley-Bockelmann 2006) that the scale height for the binary population may be much higher ($z_0 \sim 200$ pc) than that used in Hils et al. (1990).

The Hils & Bender (2000) curve is a modified result based on Hils et al. (1990), who, in calculating the GR amplitude in 1990, used too low of a space-density estimate for double WDs. In the original study of Hils et al. (1990), which neglected RLOF systems, Galactic double WDs begin to dominate the GR amplitude at ~ 0.1 mHz, and continue to dominate until ~ 1.6 mHz, where the average number of sources per resolvable frequency bin drops below 1 (similar results for the transition frequency were found in their study that included RLOF systems; Hils & Bender 2000). The analytical study of Hils et al. (1990) was not directly comparable to more recent studies of the *LISA* foreground, which utilized more sophisticated techniques. Timpano et al. (2006) performed a recalculation of the analytical Hils et al. (1990) GR foreground for Galactic binaries in order to compare the results directly to those of Nelemans et al. (2001b;

Timpano et al. 2006, see their Figure 10). Little was known about the true space density of double WDs at the time of the Hils et al. (1990) study, and since Timpano et al. (2006) was based on these results that underestimated the space density (and hence total number) of Galactic WD binaries, the Timpano et al. (2006) study had a 90% decrease in source density as compared to the study of Nelemans et al. (2001b). This reduction in number of systems resulted in a decrease in the foreground GR amplitude. Until more recent observations of double WDs were available to better constrain the space density (Warner 1995b; Roelofs et al. 2007b), the error went undetected for some time, as this decrease was serendipitously counteracted by an increase in amplitude imposed by the (too) large double WD chirp masses used in the Hils et al. (1990) and Timpano et al. (2006) studies. In short, the studies of Timpano et al. (2006, recalculated Hils et al. 1990 and Nelemans et al. 2001b) have comparable foreground levels, albeit for different physical reasons. An increased number of observations of WD binaries since the time of the Hils et al. (1990) study (i.e., SPY project; Napiwotzki et al. 2004; Anderson et al. 2005) have confirmed that the (lower) WD masses used by Nelemans et al. (2001b) coincide more closely with the masses of WDs in binaries, whereas the masses used in Hils et al. (1990) do not (see also Nelemans 2003b; Timpano et al. 2006, for further discussion).

Based on Evans et al. (1987), Nelemans et al. (2001b) used the criterion that the transition frequency occurs when the average number of binaries per bin drops below 1, and they found the transition at ~ 1.6 mHz. They also found that 12,124 detached double WDs will be resolved with *LISA*, assuming all systems above the *LISA* sensitivity limit (an S/N of 1) are detectable. In their study, which included AM CVn systems, Nelemans et al. (2004) found a transition frequency closer to ~ 2 mHz, and that a total of $\sim 22,000$ Galactic double WDs (half detached and half RLOF) would be resolvable. For an S/N of 1, we find that $\sim 43,000$ double WDs with GR frequencies <0.01 Hz are potentially resolvable with *LISA*. However, in order to perform a reasonable comparison with Nelemans et al. (2001b), we need to consider only those binaries whose GR frequencies are above ~ 2 mHz (and below 0.01 Hz; see Section 4). In this case, we find that $\sim 25,000$ double WDs may be resolvable with *LISA*.

In previous studies, it was assumed that the level of the Galactic foreground will not contribute above the frequency at which the average number of sources per bin drops below 1 (coined the "transition frequency"). Since those studies do not calculate the GR signal beyond the transition frequency, above ~ 2 mHz, their results cannot be compared with ours. We find that the frequency at which the WD foreground drops below the instrumental noise level (~ 6–8 mHz) is above the transition frequency that was found in previous studies. In contrast to previous work, it is expected that at higher frequencies ($\gtrsim 3$ mHz) the RLOF systems may contribute more significantly to the *LISA* signal than the detached systems. This has implications for the "transition frequency" between unresolved and resolved systems: the transition frequency is shifted to higher frequencies with the addition of RLOF systems.

Since we do not follow the evolution of non-degenerate stars in our *LISA* calculations, the binaries involving "pre"-hydrogen WD donors (i.e., CVs) are not shown on the figures, though we note they would make some contribution to the *LISA* data stream. We do not include the "BDs" in our *LISA* signal populations, though we note that binaries involving these BDs will not contribute significantly to the Galactic gravitational wave background as these binaries have very low chirp masses.

---

[17] We find $\sim 5 \times 10^8$ double WDs in the Milky Way.

Since the formation of such objects takes on average several Gyr, it is, however, important to include them when considering very old stellar populations such as the Galactic halo (Ruiter et al. 2009), where these systems comprise over 70% of the entire remnant binary population. In that work, it was found that the *LISA* GR signal from halo WDs will be at least an order of magnitude below the signal arising from Galactic (disk + bulge) WD binaries.

6. SUMMARY AND CONCLUSIONS

We have used the population synthesis binary evolution code `StarTrack` and the detailed *LISA* simulator of Benacquista et al. (2004) to calculate the gravitational wave foreground arising from close WD binaries in the MW disk and bulge. Our population synthesis includes both detached and mass-transferring binaries, and it is found that the mass-transferring (RLOF) binaries begin to contribute significantly to the foreground noise at high GR frequencies ($\gtrsim 3$ mHz; Figure 10, bottom panel).

Our results are in general agreement with the analytical study of Hils & Bender (2000) and the population synthesis study of Nelemans et al. (2004) for the low-frequency regime: the *LISA* signal is dominated by detached binaries. However, in contrast to previous studies, it is found that, despite the fact that the "transition frequency" is found to be $\sim$2.4 mHz using the three-bin rule of thumb, at frequencies above $\sim$3 mHz the presence of RLOF binaries will likely make it difficult to resolve individual sources, and we find that the *Galactic foreground dominates the LISA noise up to at least* $\sim$6 mHz. This is because the RLOF binaries add to the total number of *LISA* systems at high frequencies, and at high frequencies the RLOF systems chirp backward and spread out over more frequency bins, which offers a new set of challenges for *LISA* data analysts. The details of the true orbital period evolution due to mass transfer and possible tidal effects (e.g., Deloye & Bildsten 2003; Bildsten et al. 2006) are not well understood, and this uncertainty may impact the ability of future data analysis schemes to successfully resolve these systems (Arnaud et al. 2007). It is starting to become clear that such effects should be taken into account when studying the population of compact binaries (Racine et al. 2007). One new and interesting result of our study is the possibility that RLOF systems that have recently entered the mass-transfer phase (small periods, higher chirp masses) can add to the confusion foreground at higher frequencies than were previously predicted for the double WD population.

It should be repeated here that in this study, we employed one model prescription of CE evolution. This important phase of binary evolution may have a large impact on a synthesized stellar population, and various model prescriptions of CE may lead to a different number of Galactic binaries and binary physical properties, which in turn affect the shape and strength of the *LISA* GR signal. The number of close (*LISA*) binaries could potentially be decreased if the CE efficiency is low (more mergers) or if angular momentum balance rather than energy balance is assumed during the CE phase. It was shown in Ruiter et al. (2006) that when an angular momentum balance prescription is adopted (Nelemans & Tout 2005), post-CE orbital separations are overall larger, and fewer binaries will enter a CV-like RLOF phase between a white dwarf and an MS star, which is a crucial step for some of the older (bulge COHe-R2) *LISA* binaries.

We have shown that there is a large population of potentially resolvable binaries in the Galaxy. The approach of esti-

mating resolvable systems described in Section 4.3 ("S/N $\geqslant 5$" method), relies on assuming that signals arising from individual binaries are separable, i.e., can be demodulated using some sort of matched filtering technique (see Seto 2002 and references therein). If detected, once their properties are measured these systems may aid in solving several remaining problems in binary evolution theory. Especially interesting would be the detection of any double WD binary with a mass close to or over the Chandrasekhar mass (potential SN Ia progenitor or possible pre-NS accretion induced collapse object), or the measurement of the orbital periods of systems that have just emerged from a CE (the phase that determines the formation of most compact object binaries). However, we reiterate that the detection of resolvable binaries will depend on the development of sensitive detection schemes and data analysis techniques.

REFERENCES

Abbott, B., et al. (The LIGO Scientific Collaboration) 2007, ApJ, 659, 918
Abbot, B., et al. (The LIGO Scientific Collaboration) 2009, Phys. Rev. D, 80, 102001
Abt, H. A. 1983, ARA&A, 21, 343
Anderson, S. F., et al. 2005, AJ, 130, 2230
Arnaud, K. A., et al. 2007, Class. Quantum Grav., 24, 529
Beer, M. E., Dray, L. M., King, A. R., & Wynn, G. A. 2007, MNRAS, 375, 1000
Belczynski, K., Benacquista, M., & Bulik, T. 2008a, arXiv:0811.1602
Belczynski, K., Bulik, T., & Ruiter, A. J. 2005, ApJ, 629, 915
Belczynski, K., Kalogera, V., & Bulik, T. 2002, ApJ, 572, 407
Belczynski, K., Kalogera, V., Rasio, F. A., Taam, R. E., Zezas, A., Bulik, T., Maccarone, T. J., & Ivanova, N. 2008b, ApJS, 174, 223
Belczynski, K., & Taam, R. E. 2004, ApJ, 616, 1159
Benacquista, M. 2001, in AIP Conf. Proc. 586, 20th Texas Symp.: Relativistic Astrophysics, ed. J. C. Wheeler & H. Martel (Melville, NY: AIP), 793
Benacquista, M. J., DeGoes, J., & Lunder, D. 2004, Class. Quantum Grav., 21, 509
Benacquista, M., & Holley-Bockelmann, K. 2006, ApJ, 645, 589
Benacquista, M. J., Larson, S. L., & Taylor, B. E. 2007, Class. Quantum Grav., 24, 513
Bildsten, L., Townsley, D. M., Deloye, C. J., & Nelemans, G. 2006, ApJ, 640, 466
Burgay, M., et al. 2003, Nature, 426, 531
Cooray, A. 2004, MNRAS, 354, 25
Cooray, A., Farmer, A. J., & Seto, N. 2004, ApJ, 601, L47

Cornish, N. J. 2001, Phys. Rev. D, 65, 022004
Cox, A. N. (ed.) 2000, Allen's Astrophysical Quantities (4th ed., New York: Springer)
Cutler, C. 1998, Phys. Rev. D, 57, 7089
Danzmann, K. 1996, Class. Quantum Grav., 13, 247
de Kool, M. 1990, ApJ, 358, 189
Deloye, C. J., & Bildsten, L. 2003, ApJ, 598, 1217
Deloye, C. J., Taam, R. E., Winisdoerffer, C., & Chabrier, G. 2007, MNRAS, 381, 525
Duquennoy, A., & Mayor, M. 1991, A&A, 248, 485
Edlund, J. A., Tinto, M., Królak, A., & Nelemans, G. 2005, Phys. Rev. D, 71, 122003
Evans, C. R., Iben, I. J., & Smarr, L. 1987, ApJ, 323, 129
Farmer, A. J., & Phinney, E. S. 2003, MNRAS, 346, 1197
Flanagan, É. É., & Hughes, S. A. 1998, Phys. Rev. D, 57, 4535
Gair, J. R 2009, Class Quantum Grav., 26, 094034
Hils, D., & Bender, P. L. 2000, ApJ, 537, 334
Hils, D., Bender, P. L., & Webbink, R. F. 1990, ApJ, 360, 75
Hughes, S. A. 2006, in AIP Conf. Proc. 873, Laser Interferometer Space Antenna: 6th Int. *LISA* Symp., ed. S. M. Merkowitz & J. C. Livas (Melville, NY: AIP), 13
Hurley, J. R., Pols, O. R., & Tout, C. A. 2000, MNRAS, 315, 543
Iben, I., Jr., & Tutukov, A. V. 1984, ApJS, 54, 335
Kalogera, V., et al. 2004, ApJ, 601, L179
King, A. R., & Kolb, U. 1995, ApJ, 439, 330
Klypin, A., Zhao, H., & Somerville, R. S. 2002, ApJ, 573, 597
Kosenko, D. I., & Postnov, K. A. 1998, A&A, 336, 786
Kroupa, P., Tout, C. A., & Gilmore, G. 1993, MNRAS, 262, 545
Larson, S. L. 2000, Online Sensitivity Curve Generator, http://www.srl.caltech.edu/~shane/sensitivity/ (based on Larson et al. 2000)
Larson, S. L., Hiscock, W. A., & Hellings, R. W. 2000, Phys. Rev. D, 62, 062001
Lipunov, V. M., Postnov, K. A., & Prokhorov, M. E. 1987, A&A, 176, L1
Lorén-Aguilar, P., Guerrero, J., Isern, J., Lobo, J. A., & García-Berro, E. 2005, MNRAS, 356, 627
Majewski, S. R., & Siegel, M. H. 2002, ApJ, 569, 432
Marsh, T. R., Nelemans, G., & Steeghs, D. 2004, MNRAS, 350, 113
Mazeh, T., Goldberg, D., Duquennoy, A., & Mayor, M. 1992, ApJ, 401, 265
Mironovskii, V. N. 1965, AZh, 42, 977
Napiwotzki, R., et al. 2004, in ASP Conf. Ser. 318, Spectroscopically and Spatially Resolving the Components of the Close Binary Stars, ed. R. W. Hilditch, H. Hensberge, & K. Pavlovski (San Francisco, CA: ASP), 402
Nelemans, G. 2003a, Class. Quantum Grav., 20, 81
Nelemans, G. 2003b, in AIP Conf. Proc. 686, The Astrophysics of Gravitational Wave Sources, ed. J. M. Centrella & S. Barnes (Melville, NY: AIP), 263

Nelemans, G. 2009, Class. Quantum Grav., 26, 094030
Nelemans, G., Portegies Zwart, S. F., Verbunt, F., & Yungelson, L. R. 2001a, A&A, 368, 939
Nelemans, G., & Tout, C. A. 2005, MNRAS, 356, 753
Nelemans, G., Yungelson, L. R., & Portegies Zwart, S. F. 2001b, A&A, 375, 890
Nelemans, G., Yungelson, L. R., & Portegies Zwart, S. F. 2004, MNRAS, 349, 181
Nelemans, G., Yungelson, L. R., Portegies Zwart, S. F., & Verbunt, F. 2001, A&A, 365, 491
O'Shaughnessy, R., Kim, C., Kalogera, V., & Belczynski, K. 2008, ApJ, 672, 479
Peters, P. C. 1964, Phys. Rev., 136, 1224
Podsiadlowski, P. 2008, in ASP Conf. Ser. 391, Hydrogen-deficient Stars, ed. K. Werner & T. Rauch (San Francisco, CA: ASP), 323
Postnov, K. A., & Prokhorov, M. E. 1998, ApJ, 494, 674
Postnov, K. A., & Yungelson, L. R. 2006, Living Rev. Relativ., 9, 6
Racine, É., Phinney, E. S., & Arras, P. 2007, MNRAS, 380, 381
Roelofs, G. H. A., Groot, P. J., Benedict, G. F., McArthur, B. E., Steeghs, D., Morales-Rueda, L., Marsh, T. R., & Nelemans, G. 2007a, ApJ, 666, 1174
Roelofs, G. H. A., Nelemans, G., & Groot, P. J. 2007b, MNRAS, 382, 685
Rubbo, L. J., Cornish, N. J., & Poujade, O. 2004, Phys. Rev. D, 69, 082003
Ruiter, A. J. 2009, PhD thesis, New Mexico State Univ.
Ruiter, A. J., Belczynski, K., Benacquista, M., & Holley-Bockelmann, K. 2009, ApJ, 693, 383
Ruiter, A. J., Belczynski, K., & Harrison, T. E. 2006, ApJ, 640, L167
Sesana, A., Haardt, F., Madau, P., & Volonteri, M. 2005, ApJ, 623, 23
Seto, N. 2002, MNRAS, 333, 469
Smak, J. 1967, Acta Astron., 17, 255
Saio, H., & Nomoto, K. 2004, ApJ, 615, 444
Stroeer, A., & Nelemans, G. 2009, MNRAS, 400, L24
Stroeer, A., Vecchio, A., & Nelemans, G. 2005, ApJ, 633, L33
Takahashi, R., & Seto, N. 2002, ApJ, 575, 1030
Timpano, S. E., Rubbo, L. J., & Cornish, N. J. 2006, Phys. Rev. D, 73, 122001
van der Sluys, M. V., Verbunt, F., & Pols, O. R. 2006, A&A, 460, 209
Vecchio, A., & Wickham, E. D. 2004, Phys. Rev. D, 70, 082002
Wang, Z., & Chakrabarty, D. 2004, ApJ, 616, L139
Warner, B. 1995a, Ap&SS, 225, 249
Warner, B. 1995b, Cataclysmic Variable Stars (Cambridge: Cambridge Univ. Press)
Webbink, R. F. 1984, ApJ, 277, 355
Willems, B., Vecchio, A., & Kalogera, V. 2008, Phys. Rev. Lett., 100, 041102
Williams, G. 2008, Master's thesis, Univ. Texas at Browsville
Yoon, S.-C., & Langer, N. 2005, A&A, 435, 967